

# Recommendations for the echocardiographic assessment of native valvular regurgitation: an executive summary from the European Association of Cardiovascular Imaging

**Patrizio Lancellotti<sup>1\*</sup>, Christophe Tribouilloy<sup>2</sup>, Andreas Hagendorff<sup>3</sup>, Bogdan A. Popescu<sup>4</sup>, Thor Edvardsen<sup>5</sup>, Luc A. Pierard<sup>1</sup>, Luigi Badano<sup>6</sup>, and Jose L. Zamorano<sup>7</sup>, On behalf of the Scientific Document Committee of the European Association of Cardiovascular Imaging: Thor Edvardsen, Oliver Bruder, Bernard Cosyns, Erwan Donal, Raluca Dulgheru, Maurizio Galderisi, Patrizio Lancellotti, Denisa Muraru, Koen Nieman, Rosa Sicari, Document reviewers: Erwan Donal, Kristina Haugaa, Giovanni La Canna, Julien Magne, Edyta Plonska**

<sup>1</sup>Department of Cardiology, GIGA Cardiovascular Sciences, University of Liège Hospital, Valvular Disease Clinic, CHU Sart Tilman, Liège 4000, Belgium; <sup>2</sup>Department of Cardiology, University Hospital of Amiens, Picardie, France; <sup>3</sup>Department für Innere Medizin, Kardiologie, Leipzig, Germany; <sup>4</sup>Eurocolab, 'Carol Davila' University of Medicine and Pharmacy, Institute of Cardiovascular Diseases, Bucharest, Romania; <sup>5</sup>Department of Cardiology and Center for Cardiologial Innovation, Oslo University Hospital, Rikshospitalet and University of Oslo, Oslo, Norway; <sup>6</sup>Department of Cardiac, Thoracic and Vascular Sciences, University of Padova, Padova, Italy; and <sup>7</sup>University Hospital Ramón y Cajal, Madrid, Spain

Received 7 May 2013; accepted after revision 12 May 2013

Valvular regurgitation represents an important cause of cardiovascular morbidity and mortality. Echocardiography has become the primary non-invasive imaging method for the evaluation of valvular regurgitation. The echocardiographic assessment of valvular regurgitation should integrate the quantification of the regurgitation, assessment of the valve anatomy and function, as well as the consequences of valvular disease on cardiac chambers. In clinical practice, the management of patients with valvular regurgitation thus largely integrates the results of echocardiography. It is crucial to provide standards that aim at establishing a baseline list of measurements to be performed when assessing regurgitation.

**Keywords** Valvular regurgitation • Echocardiography • Recommendations • Aortic valve • Mitral valve • Tricuspid valve • Pulmonary valve

## Introduction

Doppler echocardiography is critical to initial and longitudinal assessment of patients with valvular regurgitation. It provides detailed anatomic and functional information and clarifies the mechanisms that play a role in valvular regurgitation. Doppler echocardiography not only detects the presence of regurgitation, but also permits to understand mechanisms of regurgitation, quantification of its severity, and repercussions.<sup>1–3</sup> In clinical practice, the management of patients with valvular regurgitation largely integrates the results of echocardiography. It is thus crucial to provide standards that aim at establishing a baseline list of measurements to be performed when assessing regurgitation. Practically, the evaluation of valvular regurgitation

requires the use of different echocardiographic modalities, should integrate multiple parameters, and should be combined with clinical data. The present document aims to present an executive summary of the recommendations papers published in the *European Journal of Echocardiography* on the assessment of native valvular regurgitation.<sup>2,3</sup>

## General recommendations

Two-dimensional (2D) transthoracic echocardiography (TTE) is recommended as first-line imaging in valvular regurgitation and is often sufficient for diagnosis. Two-dimensional transoesophageal

\* Corresponding author. Tel: +32 436671 94; fax: +32 436671 95, Email: plancellotti@chu.ulg.ac.be

Published on behalf of the European Society of Cardiology. All rights reserved. © The Author 2013. For permissions please email: journals.permissions@oup.com

echocardiography (TOE) is indicated when TTE is insufficient or when further diagnostic refinement is required. Three-dimensional (3D) echocardiography provides realistic and intuitive anatomic images of valvular apparatus, which may provide additional information, particularly in patients with complex valve lesions, and allows more accurate quantitation of haemodynamic consequences of the regurgitation on cardiac chambers.<sup>4</sup>

#### Valve assessment: recommendations

1. TTE is recommended as the first-line imaging modality in valvular regurgitation.
2. TOE is advocated when TTE is of non-diagnostic value or when further diagnostic refinement is required.
3. Three-dimensional echo can provide additional information in patients with complex valve lesions.
4. TOE is not indicated in patients with a good-quality TTE except in the operating room when a valve surgery is performed.

In practice, the evaluation of valvular regurgitation starts with 2D TTE, which can orient readily to a severe regurgitation in the presence of a major valvular defect or to a minor leak when the valve anatomy and leaflet motion are normal. The aetiology (cause of the valve disease) and mechanism of the regurgitation (lesion/deformation resulting in valve dysfunction) including the dysfunction type (cusp motion abnormality) are described according to the Carpentier's classification of leaflet motion: Type I: normal leaflet motion, Type II: excessive motion, and Type III: restrictive motion.<sup>5</sup>

Then, a careful assessment of the *regurgitant jet* by colour Doppler, using multiple views, can rapidly diagnose minimal regurgitation, which requires a priori no further quantification. In the other cases, the use of a more quantitative method is advised when feasible [vena contracta (VC); proximal isovelocity surface area (PISA)].

#### Estimation of the severity of valvular regurgitation: recommendations

1. The colour flow area of the regurgitant jet is not recommended to quantify the severity of valvular regurgitation.
2. Both VC measurement and the PISA method are recommended to evaluate the severity of regurgitation when feasible.
3. Adjunctive parameters should be used when there is discordance between the quantified degree of regurgitation and the clinical context.

In the second step, the impact of the regurgitation on the ventricles, the atria, and the pulmonary artery pressures is estimated. Ventricular sizes and function are measured using diameters and/or volumes (the biplane 2D method of discs or 3D echo when imaging is of proper quality) (Figure 1). Of note, ejection fraction is load dependent and often overestimates ventricular systolic performance. New parameters (myocardial velocities, myocardial deformation by 2D strain, or strain rate) are currently available for a better assessment of ventricular function, but they still need to be validated in larger series of patients in the setting of valvular regurgitation. Atrial volumes can be reliably measured by the biplane area-length method or 3D

echocardiography. The mode of acquisition, advantages, and limitations of the various echo Doppler parameters used for the assessment of valvular regurgitation severity are detailed in Tables 1 and 2. Finally, the collected data are compared with the individual clinical context in order to stratify the management and the follow-up.<sup>6</sup> When indicated for left-sided valves, a quantitative exercise echocardiography could help identify what might otherwise be considered as a moderate valvular lesion as well as the ventricular and pulmonary consequences of the regurgitation. The use of stress echocardiography in valvular heart disease is the subject of a different document.<sup>7</sup> According to the clinical context and the grade of regurgitation, *appropriate monitoring* will be delivered.<sup>6</sup>

#### LV size and function: recommendations

1. The quantitative assessment of left ventricular (LV) diameters, volumes, and ejection fraction is mandatory.
2. The 2D measurement of LV diameters is strongly advocated if the M-mode line cannot be placed perpendicular to the long-axis of the LV.
3. The 2D-based biplane summation method of discs is the recommended approach for the estimation of LV volumes and ejection fraction.
4. The 3D echo assessment of LV function provides more accurate and reproducible data.
5. Contrast echo is indicated in patients with poor acoustic window.
6. The qualitative assessment of LV function is not recommended.
7. Left atrial volume is the recommended parameter to assess its size.

## Aortic regurgitation

Aortic regurgitation (AR) is a common valvular disease. Echocardiography plays a valuable role in the assessment and management of patients with AR.<sup>1–3</sup>

### Anatomy and function of the aortic valve

The aortic valve consists of a complex of structures surrounding the aortic orifice along the outflow tract of the left ventricle (LV).<sup>8</sup> Typically, the valve has three leaflets, which are semi-lunar in shape. The cusps are inserted into a fibrous connective tissue sleeve, which is attached to the aorta media above (the valsalva sinuses and the sino-tubular junction). Below, the cusps are attached to the myocardium of the LV outflow tract (LVOT) and to the anterior mitral leaflet (virtual basal ring), below the anatomic ventriculo-aortic junction. Hence, the true anatomic aortic annulus is not actually the ring projected at the most basal leaflet insertion—as usually defined and measured with various imaging techniques—but a crown-like 3D structure. Of note, the size of the aortic annulus and root is influenced by inner pressure and is dynamically changing during the cardiac cycle. Each cusp is attached along its curved edge, and the cusps meet at three commissures that are equally spaced along the circumference of the sleeve at the supra-aortic ridge. In normal aortic valve, the cusps are symmetrical,

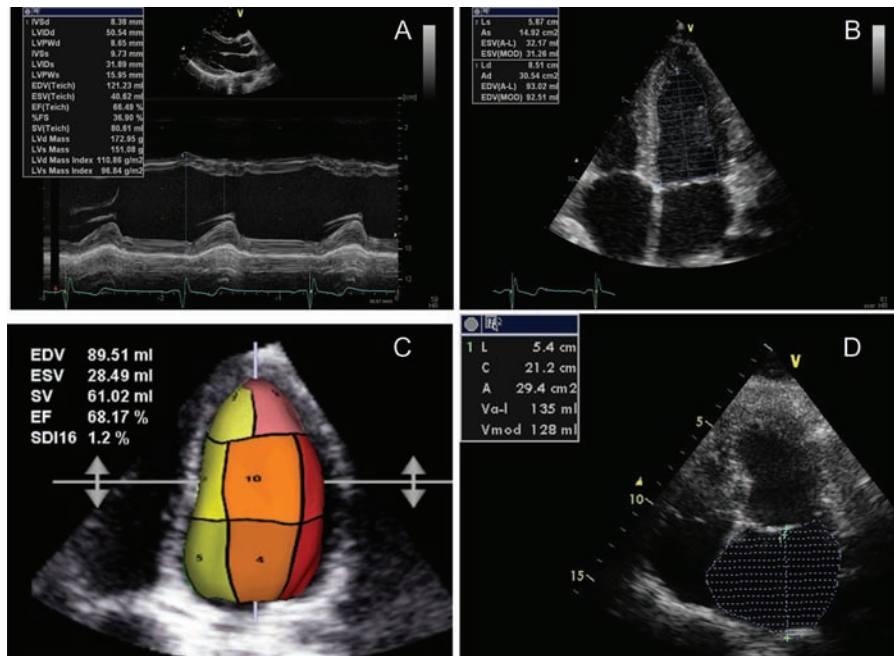


**Figure 1** (A) M-Mode measurement of LV diameters; (B) estimation of LV volumes and ejection fraction by summation method of disc; (C) 3D echo assessment of LV volumes; (D) estimation of left atrial volume by the summation method of disc.

mobile, and free at the commissures, with equal overlap on the closure. The cusps are named left, right, and non-coronary cusps based on the location of the coronary ostia.

## Aetiology and mechanisms of AR

AR results from disease of either the aortic leaflets or the aortic root that distorts the leaflets and prevents their correct apposition. Common causes of leaflet abnormalities that result in AR include senile leaflet calcifications, bicuspid aortic valve, infective endocarditis, and rheumatic fever. Aortic causes of AR include annulo-aortic ectasia (idiopathic root dilatation), Marfan's syndrome, aortic dissection, collagen vascular disease, and syphilis. The Carpentier's classification is also commonly used to describe the mechanism of AR (Figure 2) (Table 3).<sup>9</sup>

**Key point: In patients with AR, careful aortic valve analysis is mandatory. The echo report should include information about the aetiology, the lesion process, and the type of dysfunction. The likelihood of valve repair should also be discussed in case of pure AR.**

## Echocardiographic evaluation in AR

The parasternal long-axis view is classically used to measure the LV outflow tract, the aortic annulus, and the aortic sinuses dimensions. Leaflet thickness and morphology can be visualized from this window as well as from the parasternal short-axis view and the apical five-chamber view. However, not uncommonly, 2D TTE does not allow a complete assessment of the anatomy and causes of AR. In this situation, if the acoustic window is optimal, 3D echo could provide better delineation of the aortic valve morphology.<sup>4,8</sup> In some cases, TOE is needed particularly when TTE is insufficient

for assessing the mechanisms and causes of AR, as well as the aortic root dimensions and morphology.<sup>9</sup>

### Two-dimensional/M-mode findings in AR

Information about the cusp pathology (redundancy, restriction, cusp height to indicate likely adequacy of coaptation, mobility/pliability, thickness, integrity), commissure variations (fusion, splaying, attachment site, and alignment), and root morphology (septal hypertrophy, annular size, sinus and sino-tubular junction dimension, and ascending aorta dimension) should be provided. The presence of a flail valve is specific for severe AR. In addition, 2D (reverse doming of the anterior mitral valve leaflet; basal septal hyperechogenic aspect) and M-mode (high frequency fluttering of the anterior mitral leaflet, the mitral valve chordae, or the interventricular septum; premature mitral valve closure; premature diastolic opening of the aortic valve) echo findings that can be associated with AR should be looked for (Figure 3).

**Key point: Additional echo findings are used as complementary parameters to assess the severity of AR. The assessment of the morphology and dimension of the aortic root is mandatory.**

### Assessment of AR severity

#### Colour flow Doppler

**Colour flow imaging.** Using colour flow Doppler, the regurgitant jet into the LV during diastole can be visualized from multiple views. The colour jet area and length are weakly correlated to the degree of AR, are affected by the aortic to LV diastolic pressure gradient and LV compliance, and are often overestimated in the apical views. They are not currently recommended to quantitate AR severity. Practically, colour flow Doppler serves for detection and initial

**Table 1** Echocardiographic parameters used to quantify regurgitation severity: recordings

Parameters	Aortic regurgitation (AR)	Pulmonary regurgitation (PR)	Mitral regurgitation (MR)	Tricuspid regurgitation (TR)
Valve morphology	Visual assessment Multiple views	Visual assessment Multiple views	Visual assessment Multiple views	Visual assessment Multiple views
Tricuspid annulus diameter	—	—	—	Apical four-chamber view Lateral inner edge to septal inner edge
Colour flow regurgitant jet	Optimize colour gain/scale Parasternal long- and short-axis views	Optimize colour gain/scale Evaluate in parasternal short-axis view	Optimize colour gain/scale Evaluate in two views Measure blood pressure	Optimize colour gain/scale Evaluate in two views Measure blood pressure
VC width	PT-LAX is preferred (apical four-chamber view if not available) Optimize colour gain/scale Identify the three components of the regurgitant jet (VC, PISA, jet into LV) Reduce the colour sector size and imaging depth to maximize frame rate Expand the selected zone (Zoom) Use the cine-loop to find the best frame for measurement Measure the smallest VC (immediately distal to the regurgitant orifice, perpendicular to the direction of the jet)	Parasternal short-axis view Optimize colour gain/scale and identify the 3 components of the regurgitant jet Reduce the colour sector size and imaging depth to maximize frame rate Expand the selected zone (Zoom) and find the best frame for measurement Measure the smallest VC	Two orthogonal planes (PT-LAX, apical four-chamber view) Optimize colour gain/scale Identify the three components of the regurgitant jet (VC, PISA, jet into LA) Reduce the colour sector size and imaging depth to maximize frame rate Expand the selected zone (Zoom) Use the cine-loop to find the best frame for measurement Measure the smallest VC (immediately distal to the regurgitant orifice, perpendicular to the direction of the jet)	Apical four-chamber view Optimize colour gain/scale Identify the three components of the regurgitant jet (VC, PISA, jet into RA) Reduce the colour sector size and imaging depth to maximize frame rate Expand the selected zone (Zoom) Use the cine-loop to find the best frame for measurement Measure the smallest VC (immediately distal to the regurgitant orifice, perpendicular to the direction of the jet)
PISA method	Apical five-chamber for central jets (PT-LAX for eccentric jets) Optimize colour flow imaging of AR Zoom the image of the regurgitant aortic valve Increase the Nyquist limit in apical views/decrease or increase in PT-LAX With the cine-mode select the best PISA Display the colour off and on to visualize the AR orifice Measure the PISA radius at diastole using the first aliasing and along the direction of the ultrasound beam Measure AR peak velocity and TVI (CW) Calculate flow rate, EROA, R Vol	Parasternal short-axis view Optimize colour flow imaging of PR and zoom the selected region Decrease the Nyquist limit (colour flow zero baseline) Measure the PISA radius at mid-systole using the first aliasing and along the direction of the ultrasound beam Measure PR peak velocity and TVI (CW) Calculate flow rate, EROA, R Vol	Apical four-chamber Optimize colour flow imaging of MR Zoom the image of the regurgitant mitral valve Decrease the Nyquist limit (colour flow zero baseline) With the cine-mode select the best PISA Display the colour off and on to visualize the MR orifice Measure the PISA radius at mid-systole using the first aliasing and along the direction of the ultrasound beam Measure MR peak velocity and TVI (CW) Calculate flow rate, EROA, R Vol	Apical four-chamber Optimize colour flow imaging of TR Zoom the image of the regurgitant tricuspid valve Decrease the Nyquist limit (colour flow zero baseline) With the cine-mode select the best PISA Display the colour off and on to visualize the TR orifice Measure the PISA radius at mid-systole using the first aliasing and along the direction of the ultrasound beam Measure TR peak velocity and TVI (CW) Calculate flow rate, EROA, R Vol
CW regurgitant jet profile	Apical five-chamber CW AR jet	Parasternal short-axis view	Apical four-chamber	Apical four-chamber
Pressure half-time	Apical five-chamber CW AR Doppler	CW PR Doppler	—	—
Diastolic flow reversal in descending aorta	PW Doppler Proximal descending aorta/ abdominal aorta	—	—	—

Continued

**Table I Continued**

Parameters	Aortic regurgitation (AR)	Pulmonary regurgitation (PR)	Mitral regurgitation (MR)	Tricuspid regurgitation (TR)
Pulmonary vein flow	—	—	Apical four-chamber Sample volume of PW placed into the right upper pulmonary vein Interrogate the different pulmonary veins when possible	—
Hepatic vein flow	—	—	—	Subcostal view Sample volume of PW placed into the hepatic vein
Peak E velocity	—	—	Apical four-chamber Sample volume of PW placed at mitral leaflet tips	Apical four-chamber Sample volume of PW placed at tricuspid leaflet tips
Ventricular size	Use preferably the Simpson method to assess the LV	Use preferably the RV dimension from the apical four-chamber view	Use preferably the Simpson method to assess the LV	Use preferably the RV dimension from the apical four-chamber view

AR, aortic regurgitation; CW, continuous wave; EROA, effective regurgitant orifice area; LA, left atrium; LV, left ventricle; MR, mitral regurgitation; PR, pulmonary regurgitation; PT-LAX, parasternal long-axis view; PW, pulsed wave; RA, right atrium; RV, right ventricle; R Vol, regurgitant volume; TR, tricuspid regurgitation; TVI, time-velocity integral; VC, vena contracta.

visual assessment of AR. Central jets are suggestive of rheumatic disease, whereas eccentric jets are often associated with aortic valve prolapse or perforation. Colour-coded M-mode is suitable for time-course of flow signals during the heart cycle (Figure 4). The diameter and the cross-sectional area of the jet at its origin are semi-quantitative colour Doppler indexes of AR severity. The maximum colour jet diameter (width) is measured in diastole immediately below the aortic valve (at the junction of the LV outflow tract and aortic annulus) in the parasternal long-axis view. The jet width is proportional to the size of the aortic valve defect. However, since it assumes a circular regurgitant orifice, if the orifice shape is irregular, as in bicuspid valve, the colour jet width is less related to the degree of regurgitation. Its accuracy can thus be improved by normalizing the jet width for the LV outflow tract diameter. The cross-sectional area of the jet from the parasternal short-axis view and its ratio to the LV outflow tract area is also semi-quantitative parameters of AR severity. Although these measurements suffer from a high inter-observer variability, a jet width ratio >65% is a strong argument for severe AR.<sup>10</sup>

**Key point: The colour flow area of the regurgitant jet, as a single parameter, is not recommended to quantify the severity of AR. The colour flow imaging should only be used for a visual assessment of AR. A more quantitative approach is required when more than a small central AR jet is observed.**

**VC width.** For AR, imaging of the VC—the regurgitant jet as it traverses the aortic orifice or the effective regurgitant area—is obtained from the parasternal long-axis view.<sup>11–13</sup> Practically, the VC represents the smallest flow diameter at the level of the aortic valve in the LV outflow tract, immediately below the flow convergence region (Figure 5). It provides thus an estimate of the size of the effective regurgitant orifice area (EROA) and is smaller than the regurgitant jet width in the LV outflow tract (expansion of the jet immediately below the VC). Using a Nyquist limit of 50–60 cm/s, a VC width of <3 mm correlates with mild AR, whereas a width >6 mm indicates severe AR. The measurement

of the VC is affected by several factors as the presence of multiple jets. In this situation, the respective widths of the VC are not additive. The concept of VC is indeed based on the assumption that the regurgitant orifice is almost circular. The orifice is however often elliptic or irregular, which changes the width of the VC in different views. Three-dimensional colour Doppler echo has been shown to be a possible useful tool in the visualization of the actual shape of the regurgitant orifice.<sup>13</sup>

**Key point: When feasible, the measurement of the VC width is recommended to quantify AR. Intermediate VC values (3–6 mm) need confirmation by a more quantitative method, when feasible. The VC can often be obtained in eccentric jet. In case of multiple jets, the respective values of VC width are not additive. The assessment of the VC by 3D echo is still reserved for research purposes.**

**The flow convergence method.** The assessment of the flow convergence zone has been less extensively studied in AR than in mitral regurgitation (MR).<sup>14,15</sup> Imaging of the flow convergence zone is obtained from the apical three or five-chamber or parasternal long-axis or upper right parasternal views. The radius of the PISA is measured at diastole using the first aliasing. R Vol and EROA are obtained using the standard formulas (Figures 6 and 7). The flow convergence or PISA method has several limitations. Firstly, it is not feasible in a significant percentage of patients with AR due to interposition of valve tissue and difficulty in correctly identifying the flow convergence zone. Non-planar or confined flow convergence zones that invalidate the hemispheric assumption are potential causes of either under- or over-estimation of AR severity by the PISA method. Accordingly, caution should be exercised when using the PISA method in patients with obtuse flow convergence angles, such as those with aneurysmal dilation of the ascending aorta or those with confined flow convergence zone such as could occur in patients with cusp perforation or commissural leaks. Grading of the severity of AR classifies regurgitation as mild, moderate, or severe, and subclassifies the moderate regurgitation group into 'mild-to-moderate' (EROA of 10–19 mm or

**Table 2** Echocardiographic parameters used to quantify regurgitation severity: advantages and limitations

Parameters	Usefulness/advantages	Limitations
Valve morphology	Flail valve is specific for severe regurgitation (i.e. ruptured PMs in MR)	Other abnormalities are non-specific for severe valvular regurgitation
Tricuspid annulus diameter in TR	Dilatation sensitive for severe TR	Dilatation seen in other conditions Need to be confirmed in further studies
Colour flow regurgitant jet	Ease of use Evaluates the spatial orientation of regurgitant jet Good screening test for mild vs. severe regurgitation	Can be inaccurate for estimation of regurgitation severity Influenced by technical and haemodynamic factors Expands unpredictably below the orifice in AR or PR Underestimates eccentric jet adhering the atrial wall (Coanda effect) in MR or TR
VC width	Relatively quick and easy Relatively independent of haemodynamic and instrumentation factors Not affected by other valve leak Good for extremes regurgitation: mild vs. severe Can be used in eccentric jet	Not valid for multiple jets Small values; small measurement errors leads to large % error Intermediate values need confirmation Affected by systolic changes in regurgitant flow Lacks published data in PR
PISA method	Can be used in eccentric jets Not affected by the aetiology of regurgitation or other valve leak Quantitative: estimates lesion severity (EROA) and volume overload (R Vol) Flow convergence at 50 cm/s alerts to significant MR Large flow convergence at 28 cm/s alerts to significant TR	PISA shape affected by the aliasing velocity in case of non-circular orifice by systolic changes in regurgitant flow by adjacent structures (flow constraints) PISA radius is more a hemi-ellipse Errors in PISA measurement are squared Inter-observer variability Not valid for multiple jets Feasibility limited by aortic valve calcifications in AR Validated in only few studies in TR Lacks published data in PR
CW regurgitant jet profile	Simple, easily available	Qualitative, complementary finding Complete signal difficult to obtain in eccentric jet
Pressure half-time in AR or PR	Simple	Affected by LV compliance, blood pressure, acuity
Diastolic flow reversal in the descending aorta in AR	Simple	Affected by sample volume location and acuteness of AR Affected by aortic compliance. Brief velocity reversal is normal Cut-off validated for distal aortic arch
Pulmonary vein flow in MR	Simple Systolic flow reversal is specific for severe MR	Affected by LA pressure, atrial fibrillation Not accurate if MR jet is directed into the sampled vein
Hepatic vein flow in TR	Simple Systolic flow reversal is specific for severe TR	Affected by RA pressure, atrial fibrillation
Peak E velocity in MR or TR	Simple, easily available Usually increased in severe regurgitation	Affected by atrial pressure, atrial fibrillation, ventricular relaxation Complementary finding
Atrial and ventricular size	Dilatation is sensitive for chronic severe regurgitation Normal size almost excludes severe chronic regurgitation	Dilatation observed in other conditions (non-specific) May be normal in acute severe regurgitation

AR, aortic regurgitation; CW, continuous wave; EROA, effective regurgitant orifice area; MR, mitral regurgitation; PISA, proximal isovelocity surface area; PM, papillary muscle; PR, pulmonary regurgitation; RA, right atrium; R Vol, regurgitant volume; TR, tricuspid regurgitation; VC, vena contracta.

Highlighted: parameters specific to a valvular regurgitation.

a regurgitant volume, R Vol of 20–44 mL) and ‘moderate-to-severe’ (EROA of 20–29 mm<sup>2</sup> or an R Vol of 45–59 mL). An EROA  $\geq$  30 mm<sup>2</sup> or an R Vol  $\geq$  60 mL indicates severe AR.

**Key point: When feasible, the PISA method is highly recommended to quantify the severity of AR. It can be used in both central and eccentric jets. In eccentric AR jets, we recommend to use the parasternal long-axis view to evaluate the flow convergence zone. An EROA  $\geq$  30 mm<sup>2</sup> or an R Vol  $\geq$  60 mL indicates severe AR.**

#### Pulsed Doppler

*Doppler volumetric method.* The pulse wave (PW) Doppler method can be used as an alternative method to quantify the AR severity.<sup>1–3</sup> In the absence of significant MR, the mitral inflow is used to calculate the systemic stroke volume (see ‘Mitral regurgitation’ section). The pulmonary site can be used in patients with significant MR. The total stroke volume is derived from the LVOT stroke volume. This approach is time-consuming and is associated with several drawbacks. In general, a regurgitant fraction (R Vol divided by the LVOT stroke volume)  $>$  50% indicates severe AR.

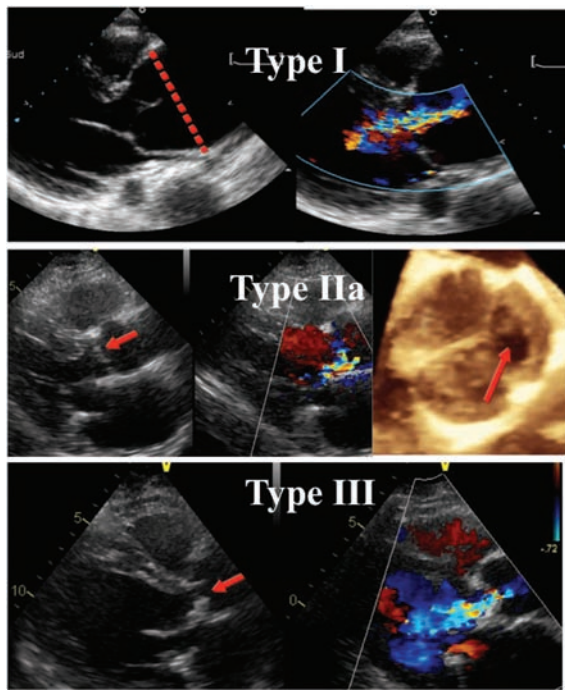


**Figure 2** Mechanisms of AR according to the Carpentier's functional classification. Type I: aortic annulus dilatation; Type IIa: prolapse of the left coronary cusp (arrow); Type III: rheumatic aortic valve disease with restricted cusp motion.

Diastolic flow reversal in the descending aorta (or peripheral arteries). AR can lead to diastolic flow reversal in the aorta. The flow reversal is best imaged in the upper descending aorta at the aortic isthmus level from a suprasternal view by using PW Doppler. The sample volume is placed just distal to the origin of the left subclavian artery and it is aligned as much as possible along the major axis of the aorta. The Doppler filter is decreased to its lowest setting to allow detection of low velocities (<10 cm/s). With milder degrees of regurgitation, there is a brief reversal of flow limited to early diastole. As the degree of the regurgitation increases, the duration and the velocity of the reversal flow during diastole increase. It becomes sustained throughout diastole at velocities exceeding 20 cm/s in severe AR (end-diastolic velocity measured at peak R-wave) (Figure 8). This cut-off value has been validated in the proximal descending aorta just beneath the aortic isthmus.<sup>16</sup> Significant holodiastolic reversal in the abdominal aorta is also a very specific sign of severe AR.

**Key point: The measurement of the diastolic flow reversal in the descending and abdominal aorta is recommended, when assessable. It should be considered as the strongest additional parameter for evaluating the severity of AR.**

#### Continuous wave Doppler of the AR jet

Continuous wave (CW) Doppler of the AR jet is classically best obtained from the apical five-chamber view (Figure 9). However, effort should be made to obtain correct Doppler angle in order to minimize errors related to possible ultrasound beam misalignment. For eccentric jets, better signals may be obtained from the right parasternal window. While faint spectral display is compatible with trace

**Table 3** Functional classification of AR lesions

Dysfunction	Echo findings
Type I: enlargement of the aortic root with normal cusps	Dilatation of any components of the aortic root (aortic annulus, sinuses of valsalva, sinotubular junction)
Type IIa: cusp prolapse with eccentric AR jet Cusp flail	Complete eversion of a cusp into the LVOT in long-axis views
Partial cusp prolapse	Distal part of a cusp prolapsing into the LVOT (clear bending of the cusp body on long-axis views and the presence of a small circular structure near the cusp free edge on short-axis views)
Whole cusp prolapse	Free edge of a cusp overriding the plane of aortic annulus with billowing of the entire cusp body into the LVOT (presence of a large circular or oval structure immediately beneath the valve on short-axis views)
Type IIb: free edge fenestration with eccentric AR jet	Presence of an eccentric AR jet without definite evidence of cusp prolapse
Type III: poor cusps quality or quantity	Thickened and rigid valves with reduced motion Tissue destruction (endocarditis) Large calcification spots/extensive calcifications of all cusps interfering with cusp motion

The degree of calcification of the aortic valve is scored as follows:  
 Grade 1: no calcification.  
 Grade 2: isolated small calcification spots.  
 Grade 3: bigger calcification spots interfering with cusp motion.  
 Grade 4: extensive calcifications of all cusps with restricted cusp motion.

or mild AR, significant overlap between moderate and severe AR exists in more dense jet tracings. Practically, the CW density does not provide useful information about the severity of AR. The grading by this method is qualitative. The rate of deceleration of the diastolic regurgitant jet and the derived pressure half-time reflect both the degree of regurgitation and the ventricular end-diastolic pressures. As the degree of AR increases, the aortic diastolic pressure decreases and the LV end-diastolic pressure increases.<sup>17,18</sup> The late diastolic jet velocity is thus reduced and the pressure half-time shortened. A pressure half-time of <200 ms is consistent with severe AR, whereas a value >500 ms suggests mild AR. Of note, the pressure half-time is however influenced by chamber compliance, the acuteness of AR (i.e. in severe acute AR, the PHT is almost always short) and the aorto-ventricular pressure gradient.

**Key point: The CW Doppler density of the AR jet does not provide useful information about the severity of AR. The assessment of the pressure half-time requires good Doppler beam alignment. A careful probe angulation is often needed. Because of the influence by chamber compliance and chamber pressures, it can only serve only as a complementary finding for the assessment of AR severity.**

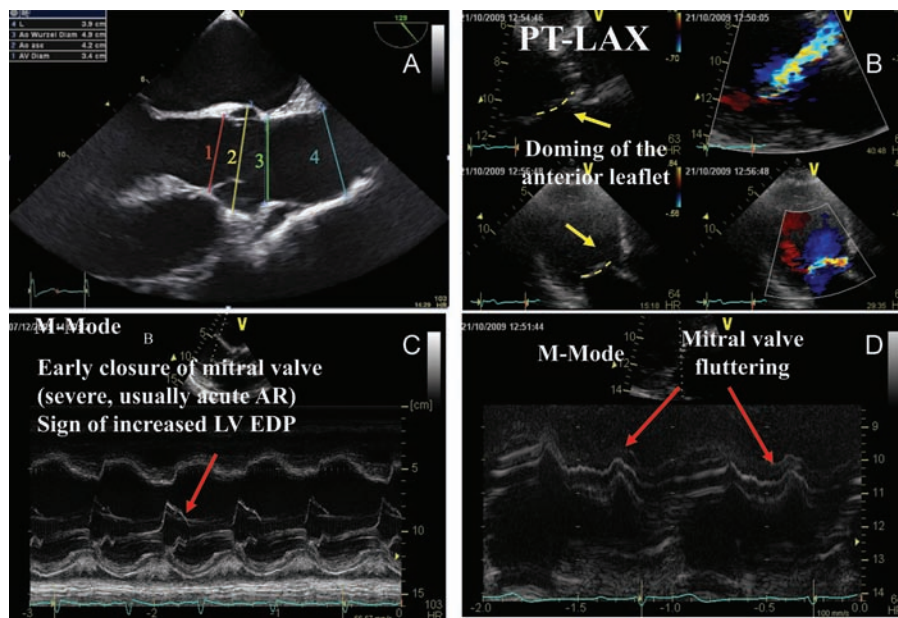


**Figure 3** (A) Measurements of the aortic diameters. (i) valve annulus, (ii) aortic sinuses, (iii) sinotubular junction, (iv) proximal ascending aorta; (B) example of AR jet impinging on the anterior mitral valve leaflet with a reverse doming of the anterior mitral valve leaflet; (C) M-mode recording showing early mitral valve closure in a patient with severe AR; (D) M-mode recording showing the fluttering motion of the anterior mitral leaflet in a patient with severe AR.

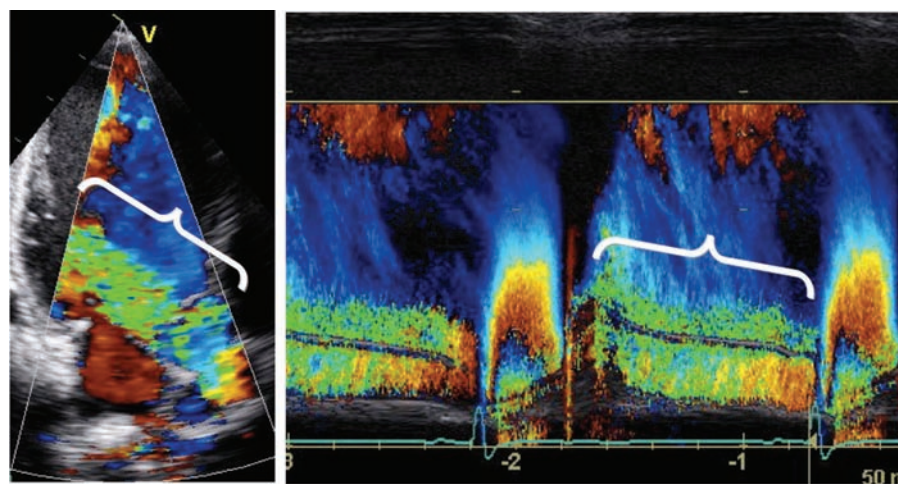


**Figure 4** (A) Colour Doppler showing a severe AR; (B) colour-coded M-mode depicting the time-dependency of flow signal during the heart cycle.

**Consequences of AR on LV size and function**

The presence of severe AR has significant haemodynamic effects, primarily on the LV. AR imposes additional volume load on the LV. In acute AR, the LV is classically not enlarged, while in the chronic situation, the LV progressively dilates and irreversible LV damage may occur. Hence, dilatation is sensitive for chronic significant AR while the normal size almost excludes severe chronic AR. However, dilatation can be observed in other conditions (non-specific) or may be absent in acute severe AR.

**Key point: LV diameters, volumes, and ejection fraction should always be measured and reported. It is strongly recommended to index the LV diameters and volumes to the body surface area.**

**Integrating indices of severity**

The echocardiographic assessment of AR includes integration of data from 2D/3D imaging of the aortic root, aortic valve, and LV as well as Doppler measures of regurgitation severity (Table 4). Effort should be made to quantify the degree of regurgitation, except in the presence



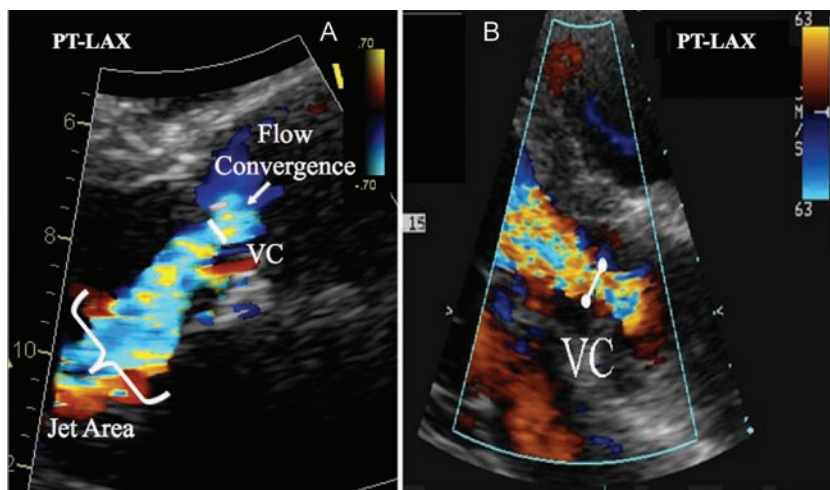


**Figure 5** (A) Semi-quantitative assessment of AR severity using the vena contracta width (VC). The three components of the regurgitant jet (flow convergence zone, vena contracta, jet turbulence) are obtained. PT-LAX: parasternal long-axis view; (B) assessment of the VC in a patient with an AR jet directed towards the septum.

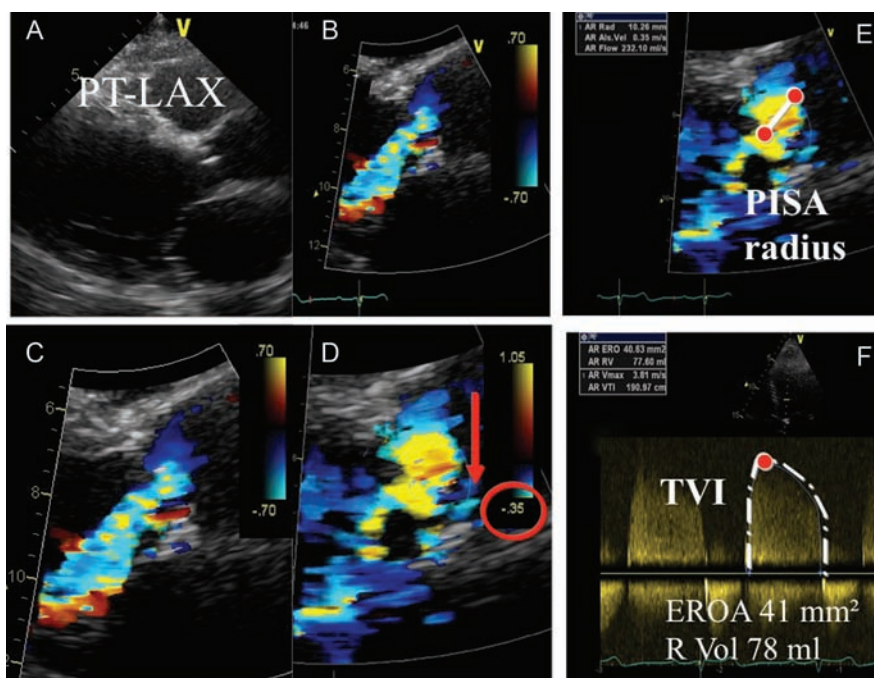
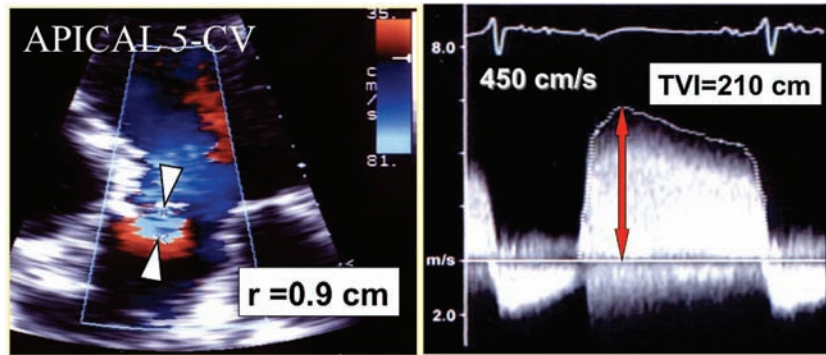


**Figure 6** Quantitative assessment of AR severity using the PISA method. Stepwise analysis of AR: (A) parasternal long-axis view (PT-LAX); (B) colour-flow display; (C) zoom of the selected zone; (D) downward shift of zero baseline to obtain a hemispheric PISA; (E) measure of the PISA radius using the first aliasing; (F) Continuous wave Doppler of AR jet allowing calculation the effective regurgitant orifice area (EROA) and regurgitant volume (R Vol). TVI, time-velocity integral.

of mild or less AR. Both the VC width and the PISA method are recommended, whenever possible. Adjunctive parameters help to consolidate about the severity of AR and should be widely used particularly when there is discordance between the quantified degree of AR and the clinical context. These parameters should be interpreted according the chronicity of AR and the LV remodelling.

### Pulmonary regurgitation

A slight amount of pulmonary regurgitation (PR) has been reported in 40–78% of patients with normal pulmonary valves. Acquired mild-to-moderate PR is most often seen in patients with pulmonary hypertension with dilatation of the pulmonary artery. Severe PR is



$$\begin{aligned} \text{EROA} &= \text{Flow} / \text{Peak velocity} \\ \text{EROA} &= (2\pi r^2 \times V_a) / \text{Peak velocity} \\ \text{EROA} &= (2 \times 3.14 \times 0.9 \times 35) / 450 \\ \text{EROA} &= 178 / 450 = 0.39 \text{ cm}^2 \\ \text{R Vol} &= \text{EROA} \times \text{TVI} \\ \text{R Vol} &= 0.39 \text{ cm}^2 \times 210 \text{ cm} = 82 \text{ mL} \end{aligned}$$

**Figure 7** Quantitative assessment of AR severity using the PISA method from the apical five-chamber view (CV). R Vol: regurgitant volume; EROA, effective regurgitant orifice area; TVI, time-velocity integral;  $V_a$ , aliasing velocity.

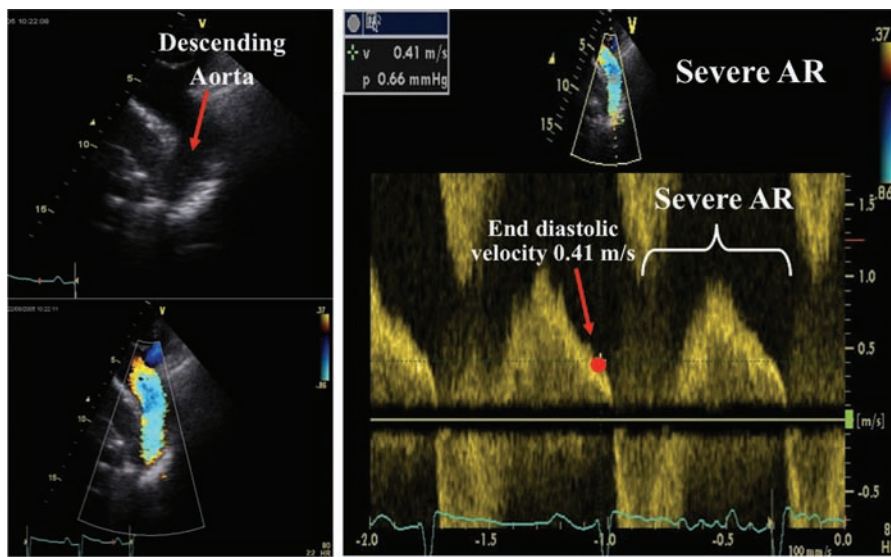


**Figure 8** A pulsed Doppler recording within the descending aorta from a patient with severe AR demonstrates flow reversal throughout diastole. An end-diastolic flow velocity  $>20$  cm/s is indicative of severe AR.

uncommon and usually observed in patients with anatomic abnormalities of the valve or after valvulotomy.<sup>19</sup> There are very few validated studies owing to the low prevalence rates and difficulties in imaging.

### Anatomy and function of the pulmonary valve

The pulmonary valve is a three leaflet structure, anatomically similar to the aortic valve (Figure 10). The pulmonic valve structure is

however thinner because of the lower pressures in the right than in the left heart system.

### Aetiology and mechanisms

Pulmonary regurgitation may be caused by congenital anomalies (quadricuspid or bicuspid valves), hypoplasia, post-repair of Tetralogy of Fallot, or prolapse of the pulmonary valve. Other causes include infective endocarditis, carcinoid syndrome, and rheumatic heart disease. Carcinoid syndrome results in shortening and

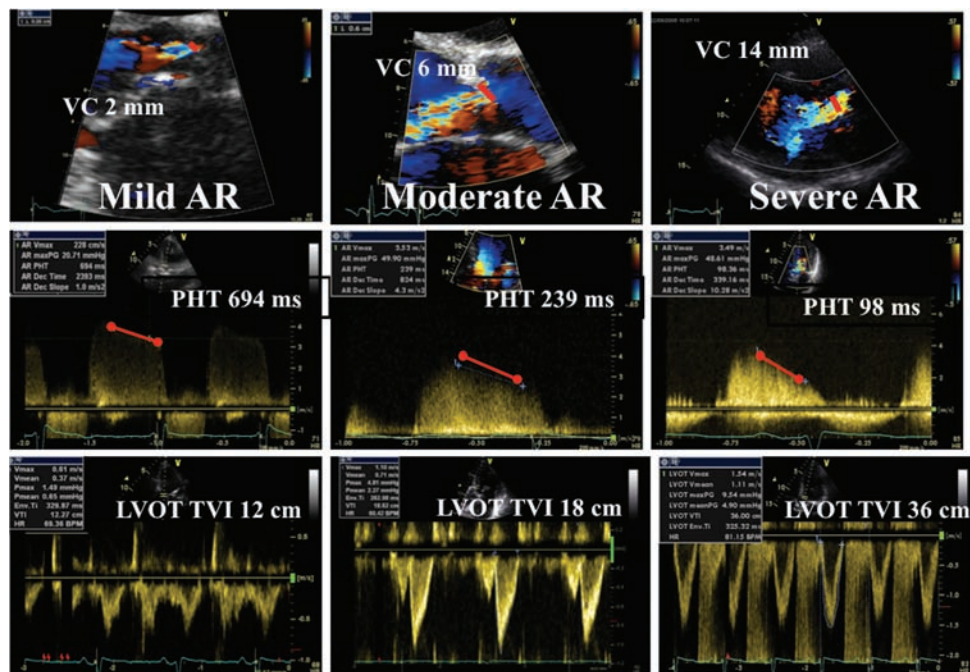


**Figure 9** Three examples of AR are provided, all taken from the parasternal long-axis view using colour Doppler (top) and from the apical five-chamber view using continuous wave Doppler (mid). The vena contracta (VC) increases with the severity of AR. The pressure half-time (PHT) decreases with more severe AR, whereas the left ventricular outflow time velocity (LVOT TVI) integral increases.

**Table 4** Grading the severity of AR

Parameters	Mild	Moderate	Severe
<b>Qualitative</b>			
Aortic valve morphology	Normal/abnormal	Normal/abnormal	Abnormal/flail/large coaptation defect
Colour flow AR jet width <sup>a</sup>	Small in central jets	Intermediate	Large in central jet, variable in eccentric jets
CW signal of AR jet	Incomplete/faint	Dense	Dense
Diastolic flow reversal in the descending aorta	Brief, protodiastolic flow reversal	Intermediate	Holodiastolic flow reversal (end-diastolic velocity > 20 cm/s)
Diastolic flow reversal in the abdominal aorta	Absent	Absent	Present
<b>Semi-quantitative</b>			
VC width (mm)	<3	Intermediate	≥6
Pressure half-time (ms) <sup>b</sup>	>500	Intermediate	<200
<b>Quantitative</b>			
EROA (mm <sup>2</sup> )	<10	10–19; 20–29 <sup>d</sup>	≥30
R Vol (mL)	<30	30–44; 45–59 <sup>d</sup>	≥60
+ LV size <sup>c</sup>			

AR, aortic regurgitation; CW, continuous wave; LA, left atrium; EROA, effective regurgitant orifice area; LV, left ventricle; R Vol, regurgitant volume; VC, vena contracta.

<sup>a</sup>At a Nyquist limit of 50–60 cm/s.

<sup>b</sup>Pressure half-time is shortened with increasing LV diastolic pressure, vasodilator therapy, and in patients with a dilated compliant aorta or lengthened in chronic AR.

<sup>c</sup>Unless for other reasons, the LV size is usually normal in patients with mild AR. In acute severe AR, the LV size is often normal. Accepted cut-off values for non-significant LV enlargement: LV end-diastolic diameter <56 mm, LV end-diastolic volume <82 mL/m<sup>2</sup>, LV end-systolic diameter <40 mm, LV end-systolic volume <30 mL/m<sup>2</sup>.

<sup>d</sup>Grading of the severity of AR classifies regurgitation as mild, moderate, or severe, and subclassifies the moderate regurgitation group into 'mild-to-moderate' (EROA of 10–19 mm<sup>2</sup> or an R Vol of 20–44 mL) and 'moderate-to-severe' (EROA of 20–29 mm<sup>2</sup> or an R Vol of 45–59 mL).

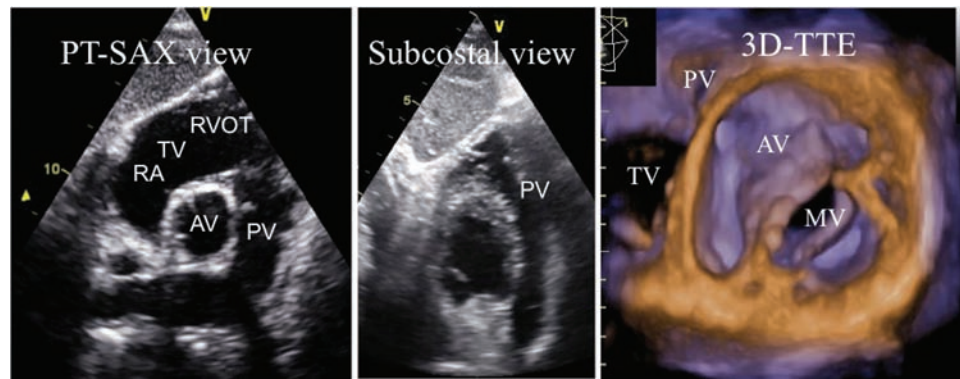


**Figure 10** Two-dimensional and 3D echo recordings of the pulmonic valve. PT-SAX, parasternal short-axis view.

thickening of the pulmonary valve leaflets, similar to the involvement of the tricuspid valve. Myxomatous valve is rare, resulting in thickening, redundancy, and sagging of the pulmonary valve leaflets.

### Echocardiographic evaluation in PR

TTE, TOE, or 3D echo could provide useful information regarding anomalies of cusp number (bicuspid or quadricuspid valves), motion (doming or prolapse), or structure (hypoplasia, dysplasia, absence of pulmonary valve). The evaluation of the pulmonary valve anatomy is, however, more difficult than for other valves (limited by poor acoustic access). With 2D echo, typically only one or two leaflets of the pulmonary valve can be simultaneously visualized. On occasion, the pulmonary valve can be seen in a short-axis view. In adults, visualization of the pulmonary valve is obtained from the parasternal short-axis view at the level of the aortic valve or from a subcostal approach. The role of TOE in PR is limited since the pulmonary valve is more difficult to image with TOE (far from the probe). The views that maximize visualization of the pulmonary valve include horizontal plane imaging at the level of the short-axis aortic valve (“inflow-outflow view”) and a deep gastric view in the 120° imaging plane (outflow view).

#### Assessment of PR severity

Determination of the PR severity has been less validated than determination of AR severity.

##### Colour flow Doppler

**Colour flow imaging.** Detection of PR relies almost exclusively on colour flow imaging. PR is diagnosed by documenting a diastolic jet in the right ventricular (RV) outflow tract directed towards the RV. Pathological PR is distinguished from physiological PR by a longer duration of flow (holodiastolic) and a wider jet as the regurgitant jet crosses the pulmonic valve.<sup>20</sup> Functional PR jets are usually very small, central, and spindle shaped. In severe PR, where equalization of the diastolic pulmonary artery and RV pressures occurs earlier in diastole, the colour jet area can be brief and inaccurate (dependency on the driving pressure).<sup>21</sup> The assessment of PR severity is usually estimated by the diameter of the jet at its origin.<sup>22</sup> The maximum colour jet diameter (width) is measured in diastole immediately below the pulmonic valve (at the junction of the RV outflow tract and pulmonary annulus) in the parasternal short-axis view or

from the subcostal view. Although this measurement suffers from a high inter-observer variability, a jet width that occupies >50–65% of the RV outflow tract width measured in the same frame suggests severe PR.<sup>23</sup>

Detection of reversal colour Doppler flow in pulmonary arteries is a very specific sign of severe PR.

**VC width.** Although the VC width is probably a more accurate method than the jet width to evaluate PR severity by colour Doppler, it lacks validation studies (Figures 11 and 12). As for other regurgitations, the same limitations are applicable. The shape of the VC is complex in most cases. The value of 3D echo has not yet been defined.<sup>24</sup>

**The flow convergence method.** In some patients, the flow convergence zone can be assessed (Figure 13). However, no studies have examined the clinical accuracy of this method in quantifying the severity of PR.

##### Pulsed Doppler

Theoretically, PW Doppler assessment of the forward and reverse flows at the pulmonary annulus and in the pulmonary artery can be used to calculate R Vol and regurgitant fraction. The pulmonary annulus should be measured carefully during early ejection (2–3 frames after the R-wave on the ECG), just below the valve. This technique is subject to errors in measurement and is not well validated.<sup>25</sup>

##### Continuous wave Doppler

There is no clinically accepted method of quantifying PR using CW Doppler. The density of the CW signal provides a qualitative measure of regurgitation.<sup>26</sup> In mild PR, there is a slow deceleration of the jet velocity. A rapid deceleration rate with termination of flow in mid-to-late diastole is not specific but compatible with severe regurgitation. In patients with congenital disease, a pressure half-time <100 ms yields good sensitivity and specificity for severe PR.<sup>27</sup> The pressure half-time is dependant not only on PR severity, but also on diastolic intrapulmonary pressures and on diastolic properties of the RV, with shorter pressure half-time when RV physiology is restrictive.

#### Consequences of PR

The evaluation of the size and function of the RV in the absence of pulmonary hypertension provides indirect clues to the severity of PR. Evidence of RV dilatation is, however, not specific for severe PR.

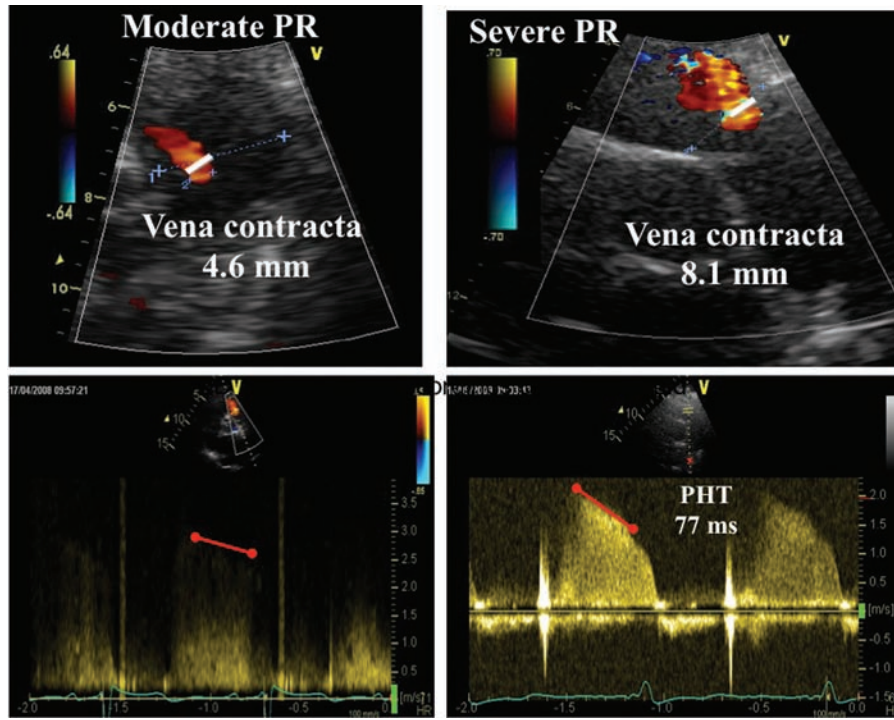


**Figure 11** Assessment of PR severity by using colour-flow imaging. Top: measurements of the right ventricular outflow tract dimension (RVOT) and regurgitant jet width in two patients with TR. Bottom: continuous wave Doppler recordings.

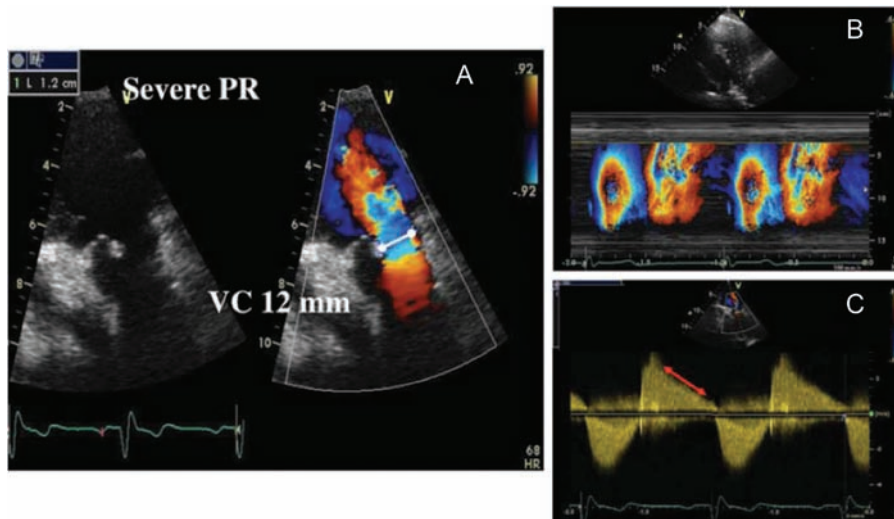


**Figure 12** Example of a patient with a severe PR: (A) left, complete lack of valve coaptation and right, the measurement of the vena contracta width (VC); (B) colour-coded M-mode depicting the time-dependency of flow signal during the heart cycle; (C) continuous Doppler recording of PR showing a rapid flow deceleration during the diastole (red arrow) and increased systolic flow velocity (not related to concomitant pulmonary stenosis).

Nevertheless, its absence suggests milder degree of PR or acute PR. Of note, dilatation can be observed in other conditions (non-specific) or may be absent in acute severe PR. As for tricuspid regurgitation

(TR), the RV function is classically evaluated by the RV volumes and the RV fractional area change. 3D echocardiography allows more accurate evaluation of RV ejection fraction than 2D. The utility of the

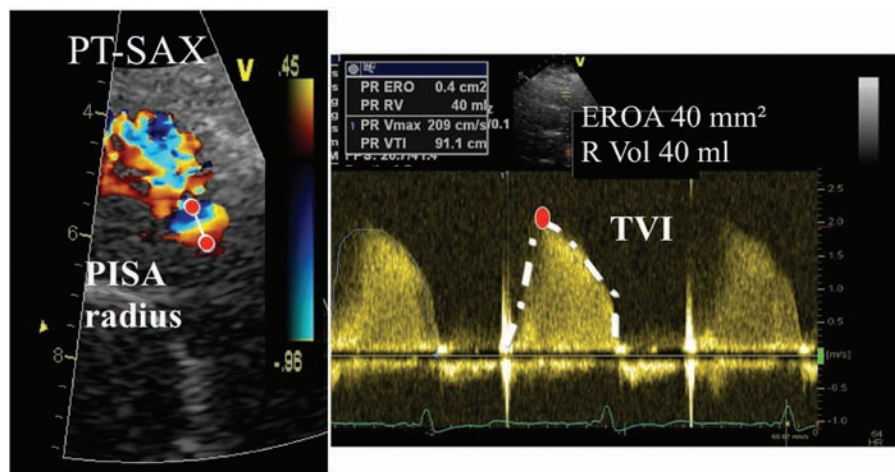


**Figure 13** Assessment of PR by the PISA method.

**Table 5** Grading the severity of PR

Parameters	Mild	Moderate	Severe
Qualitative			
Pulmonic valve morphology	Normal	Normal/abnormal	Abnormal
Colour flow PR jet width <sup>a</sup>	Small, usually <10 mm in length with a narrow origin	Intermediate	Large, with a wide origin; may be brief in duration
Reversal flow in pulmonary arteries	Absent	Absent	Present
CW signal of PR jet <sup>b</sup>	Faint/slow deceleration	Dense/variable	Dense/steep deceleration, early termination of diastolic flow
Pulmonic vs. aortic flow by PW	Normal or slightly increased	Intermediate	Greatly increased
Semi-quantitative			
VC width (mm)	Not defined	Not defined	Not defined
Pressure half-time <sup>c</sup>	Not defined	Not defined	<100 ms
Jet width ratio	Not defined	Not defined	>50–65%
Quantitative			
EROA (mm <sup>2</sup> )	Not defined	Not defined	Not defined
R Vol (mL)	Not defined	Not defined	Not defined
+RV size <sup>d</sup>			

PR, pulmonic regurgitation; CW, continuous wave; EROA, effective regurgitant orifice area; PW, pulse wave; RV, right ventricle; R Vol, regurgitant volume; VC, vena contracta.

<sup>a</sup>At a Nyquist limit of 50–60 cm/s.

<sup>b</sup>Steep deceleration is not specific for severe PR.

<sup>c</sup>Pressure half-time is shortened with increasing RV diastolic pressure.

<sup>d</sup>Unless for other reasons, the RV size is usually normal in patients with mild PR. In acute severe PR, the RV size is often normal. *Accepted cut-off values for non-significant RV enlargement (measurements obtained from the apical four-chamber view):* Mid-RV dimension  $\leq 33$  mm, RV end-diastolic area  $\leq 28$  cm<sup>2</sup>, RV end-systolic area  $\leq 16$  cm<sup>2</sup>, RV fractional area change  $> 32\%$ , maximal.

other indices deriving from tissue Doppler imaging has not been extensively examined in the context of PR unrelated to congenital heart disease.

### Integrating indices of severity

The echocardiographic assessment of PR includes integration of data from 2D/3D imaging of the pulmonary valve and RV as well as Doppler measures of regurgitation severity (Table 5). In the

absence of extensive data on the quantitation of PR, the experts recommend to assess the PR severity by using the different approaches available and to corroborate each other.

**Key point: Grading of PR severity remains difficult since standards for the quantification of PR are less robust than for AR. The VC is probably the most accurate approach. If possible, the PISA method could provide the quantitative evaluation of PR. In all cases, it is recommended to**

corroborate the results of these methods with the other available parameters.

## Mitral regurgitation

MR is increasingly prevalent in Europe despite the reduced incidence of rheumatic disease.<sup>5</sup> Echocardiography plays a key role in the assessment and management of patients with MR.

### Anatomy and function of the mitral valve

Normal mitral valve function depends on perfect function of the complex interaction between the mitral leaflets, the subvalvular apparatus (chordae tendineae, and papillary muscles), the mitral annulus, and the LV. An imperfection in any one of these components can cause the valve to leak.<sup>28</sup> The normal mitral valve has two leaflets; the posterior attached to the two-thirds of the annular plane and the anterior, to the remaining one-third. They are each divided into three scallops: A1, A2, A3 and P1, P2, P3. A1 and P1 correspond to the external, anterolateral portion of their respective leaflet, close to the anterolateral commissure, and the left atrial appendage. In opposite, A3 and P3 are internal, close the posteromedial commissure, and the tricuspid annulus.

### Aetiology and mechanisms of MR

According to aetiology, MR can be classified as primary (i.e. organic/structural: intrinsic valvular disease) or secondary (i.e. functional/non-structural: without evident structural abnormalities of the mitral valve) whereas the mechanism is based on Carpentier's classification of leaflet motion: Type I: normal leaflet motion, Type II: excessive motion, Type III: restrictive motion (A: systolic/diastolic and B: systolic) (Figure 14). Causes of primary MR include most commonly degenerative disease (Barlow, fibroelastic degeneration, Marfan, Ehlers-Danlos, annular calcification), rheumatic disease, toxic valvulopathy, and endocarditis. Ruptured papillary muscle secondary to myocardial infarction is included as primary ischaemic MR.

Degenerative disease, the most common surgical MR cause, covers a large spectrum of lesions (Figure 15): (i) isolated billowing with leaflets tips remaining intra-ventricular to flail leaflet with valvular eversion [the leaflet tip is directed towards the left atrium (LA)], (ii) isolated scallop to multi-segment (or generalized) prolapse (the leaflet tip is directed towards the LV and the coaptation line is behind the annular plane), (iii) thin/non-redundant leaflets to thick/excess tissue (Barlow's disease).

Secondary MR develops despite a structurally normal mitral valve in the context of ischaemic heart disease, dilated cardiomyopathy, or severe LA dilatation.<sup>29,30</sup> It results from an imbalance between the

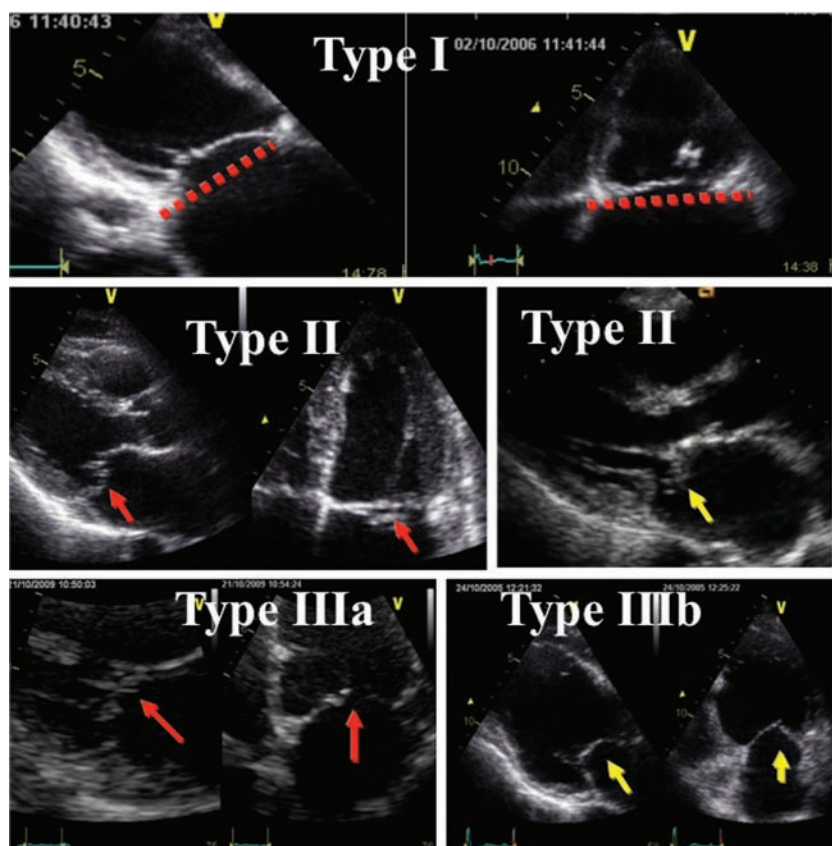
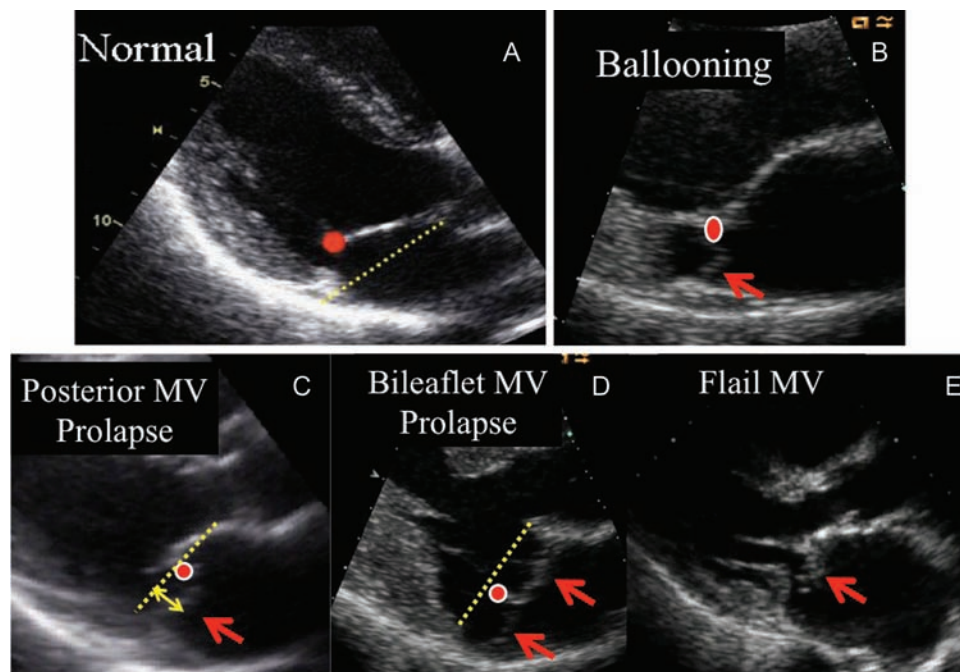


Figure 14 Mechanisms of mitral regurgitation according to the Carpentier's functional classification.



**Figure 15** (A) In normal mitral valve, the coaptation (red point) occurs beyond the mitral annular plane (line); (B) billowing mitral valve is observed when a part of the mitral valve body protrudes into the left atrium (arrow); (C and D) Mitral valve prolapse is defined as abnormal systolic displacement of 1 (C posterior prolapse) or both leaflets into the left atrium below the annular (D bileaflet prolapse); (E) flail of the anterior leaflet (arrow).

forces acting on mitral leaflets and LV-generated closing forces. LV remodelling and the resulting tethering of the mitral valve play a major role in the genesis of secondary MR. Chronic secondary ischaemic MR results, in 95% of the cases, from a type IIIb dysfunction. The restrictive motion occurs essentially during systole and is more frequent in patients with previous posterior infarction (asymmetric pattern).<sup>31</sup> In this setting, the traction on the anterior leaflet by secondary chordae can induce the so-called 'seagull sign' (Figure 16A). In patients with idiopathic dilated cardiomyopathy or with both anterior and inferior infarctions, both leaflets exhibit a reduced systolic motion leading to incomplete coaptation (symmetric pattern) (Figure 16B). Rarely, in ischaemic MR, the mechanism of MR is related to fibrosis and elongation of the papillary muscle.

*Rheumatic MR* is characterized by variable thickening of the leaflets especially at the level of their free edge. Fibrosis of the chordae is frequent, especially of those attached to the posterior valve explaining the rigidity and reduced motion of the posterior leaflet in diastole (Type IIIa).

In some patients, the posterior leaflet remains in a semi-open position throughout the cardiac cycle and the motion of the anterior leaflet in systole produces a false aspect of prolapse.

## Echocardiographic evaluation in MR

### Mitral valve morphology

Two-dimensional TTE and TOE are often used to accurately assess the mitral valve morphology (Figures 17 and 18). The TTE *parasternal short-axis* view and the TOE *transgastric* view at 0° permit the assessment of the six scallops and, with colour Doppler imaging, the

localization of the origin of the regurgitant jet may identify prolapsing segments. The TTE *parasternal long-axis* and the TOE *sagittal* view at 120° classically show A2 and P2. With TOE, angulation of the probe towards the aortic valve allows the visualization of A1 and P1 and towards the tricuspid, the visualization of A3 and P3. In *apical four-chamber* view, appreciation of A3, A2, and P1 (internal to external) is possible as the TTE *two-chamber* view or the TOE view at 40° to 60° with TOE displays P3, A2, and P1 (left to right, bi-commissural view). The precise location of the involved leaflets/scallops, the description of the presence and extent of calcifications and the extent of anatomic changes are fundamental parameters to be provided. A flail leaflet, a ruptured papillary muscle or a large coaptation defect is specific for severe MR.

Of note, with 2D TTE, the diagnosis of prolapse should be made in the parasternal or eventually the apical long-axis view, but not in the apical four-chamber view, because the saddle-shaped annulus may lead to false positive diagnosis. Using the *parasternal long-axis* TTE view, annular dilatation is identified when the ratio annulus/anterior leaflet is >1.3 (in diastole) or when the annulus diameter is >35 mm.<sup>32</sup> The normal contraction of the mitral annulus (decrease in the annular area in systole) is 25%.<sup>33</sup> When available, the 3D imaging provides a comprehensive evaluation of the mitral valve morphology (Figure 19). This technique has been shown to be superior to describe mitral pathology, especially for anterior leaflet defects and commissural involvement in degenerative disease and commissural fusion in the rheumatic process. The 'en face' view of the valve from the atrial perspective is identical to the surgical view in the operating room.<sup>8</sup>



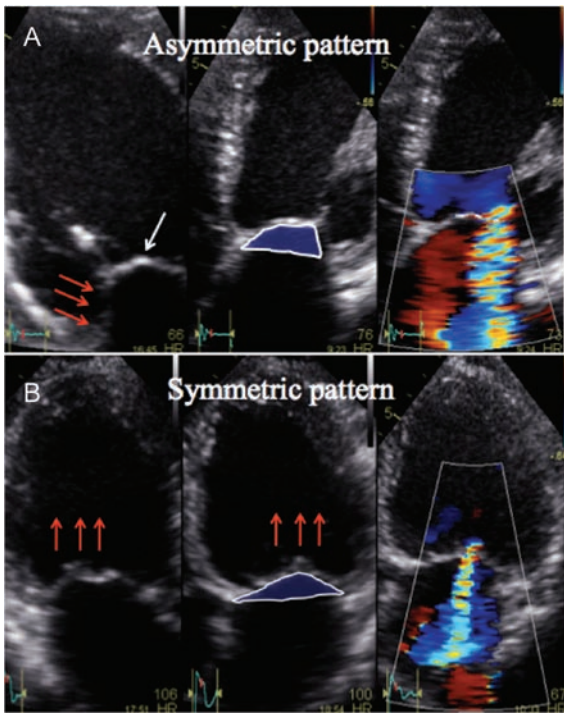


**Figure 16** (A) Ischaemic MR with a predominant posterior leaflet restriction (arrows) leading to an asymmetric tenting pattern. The restriction on the anterior leaflet due excessive stretching by the strut chordate provides the typical seagull sign (white arrow). The colour jet is originating centrally but is directed laterally towards the lateral wall of the left atrium. (B) Ischaemic MR with a bileaflet restriction (arrows) leading to a symmetric tenting pattern. The colour jet is originating and directed centrally into the left atrium.

**Predictors of successful valve repair**

Several echocardiographic parameters can help to identify patients at risk of treatment failure. In primary MR, some predictors of unsuccessful repair have been reported: the presence of a large central regurgitant jet, severe annular dilatation (>50 mm), involvement of ≥ 3 scallops especially if the anterior leaflet is involved, and extensive valve calcification (Table 6).<sup>34</sup> Moreover, the lack of valve tissue is also an important predictor of unsuccessful repair both in rheumatic valve disease and in patients who have had infective endocarditis with large valve perforation.

In secondary ischaemic MR, patients with a mitral diastolic annulus diameter ≥ 37 mm, a systolic tenting area ≥ 1.6 cm<sup>2</sup>, and a severe functional ischaemic MR could have a 50% probability of recurrence of regurgitation after mitral valve repair.<sup>35</sup> Pre-operatively (TTE), several parameters are associated with an increased risk of mitral valve repair failure (Table 7<sup>33</sup>) (Figure 20).

**Key point: The echocardiographic report should provide clues on the likelihood of valve repair.**

**Assessment of MR severity**

*Colour flow Doppler*

*Colour flow imaging.* Colour flow imaging is the most common way to assess MR severity.<sup>36</sup> The general assumption is that as the severity of the MR increases, the size and the extent of the jet into the LA also increase. Theoretically, larger colour jets that extend deep into the LA represent more MR than smaller thin jets that appear just beyond the mitral leaflets. However, the relationship between jet size and MR severity presents a large range of variability because, in addition to regurgitation severity, the colour flow display depends on many technical and haemodynamic factors. For a similar severity, patients with increased LA pressure or with eccentric jets that hug the LA wall or in whom the LA is enlarged may exhibit smaller jets area than those with normal LA pressure and size or with central jets (Figure 21).<sup>37</sup> In acute MR, even centrally directed jets may be

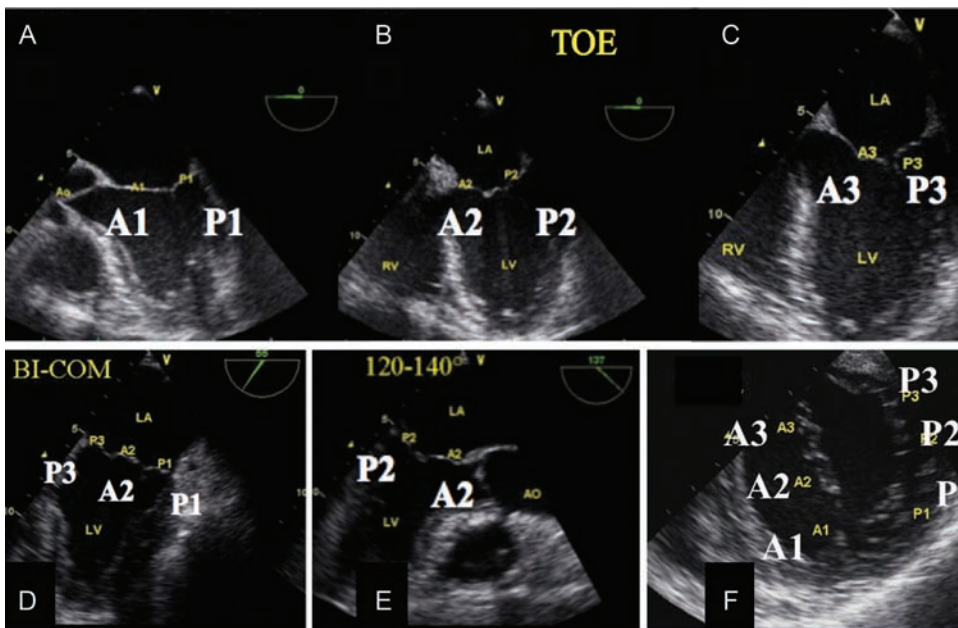


**Figure 17** Mitral valvular segmentation analysis with 2D TOE. (A, B, and C) Views obtained at 0°: (A) five-chamber view depicting A1 and P1, four-chamber view depicting A2 and P2; downwards four-chamber view depicting A3 and P3; (D) bicommissural view; (E) view at 120° visualizing A2 and P2; (F) transgastric view at 0° depicting each scallop.

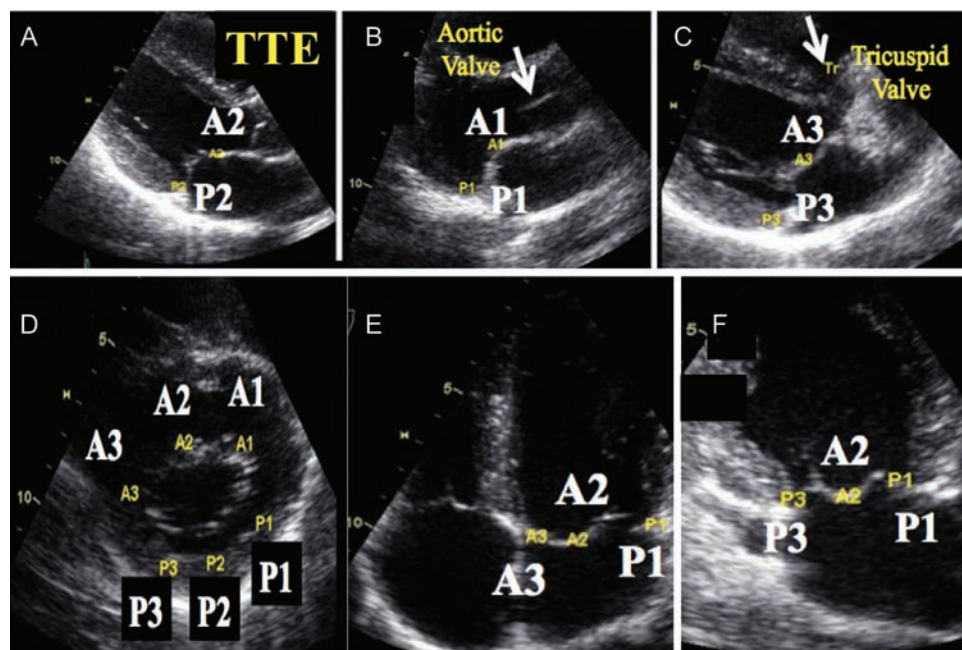


**Figure 18** Mitral valvular segmentation analysis with 2D TTE. (A) 2D TTE parasternal long-axis view depicting A2 and P2; (B) A1 and P1 (tilting of the probe towards the aortic valve); (C) A3 and P3 [tilting of the probe towards the tricuspid (Tr) valve]; (D) 2D TTE parasternal short-axis view depicting each scallop; (E) four-chamber view depicting A3, A2, and P1; (F) bicommissural view. For (B) and (D) see above.

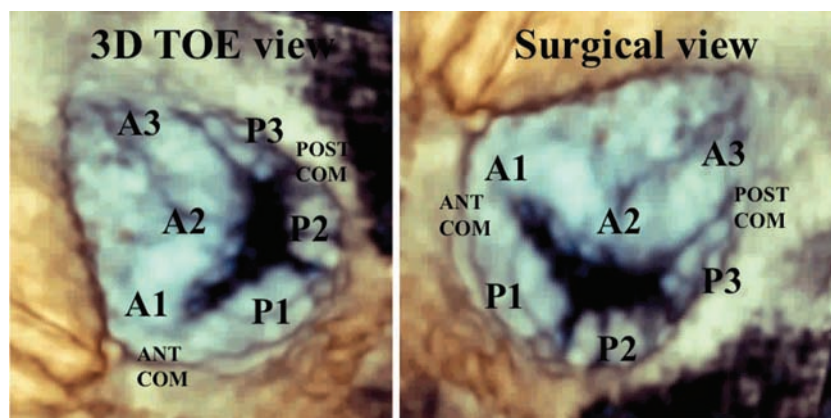


**Figure 19** Real-time 3D TOE volume rendering of the mitral valve. Left: classical TEE view; right: surgical view. A1, A2, A3: anterior mitral valve scallops; P1, P2, P3: posterior mitral valve scallops; ANT COMM: anterolateral commissure; POST COMM: posteromedial commissure.

misleadingly small. Furthermore, as this method is a source of many errors, it is not recommended to assess MR severity. Nevertheless, the detection of a large eccentric jet adhering, swirling, and reaching the posterior wall of the LA is in favour of severe MR. Conversely, small thin jets that appear just beyond the mitral leaflets usually indicate mild MR.

**Key point: The colour flow area of the regurgitant jet is not recommended to quantify the severity of MR. The colour flow imaging should only be used for detecting MR. A more quantitative approach is required when more than a small central MR jet is observed.**

VC width. The VC is the area of the jet as it leaves the regurgitant orifice; it reflects thus the regurgitant orifice area.<sup>38,39</sup> The VC is typically imaged in a view perpendicular to the commissural line (Figure 22). Averaging measurements over at least two to three beats and using two orthogonal planes, whenever possible is recommended. A VC < 3 mm indicates mild MR, whereas a width  $\geq 7$  mm defines severe MR.

The concept of VC is based on the assumption that the regurgitant orifice is almost circular. The orifice is roughly circular in primary MR; while in secondary MR, it appears to be rather elongated along the mitral coaptation line and non-circular.<sup>40,41</sup> Thus, the VC could

**Table 6** Probability of successful mitral valve repair in MR based on echo findings

Aetiology	Dysfunction	Calcification	Mitral annulus dilatation	Probability of repair
Degenerative	II: Localized prolapse (P2 and/or A2)	No/localized	Mild/moderate	Feasible
Secondary	I or IIIb	No	Moderate	Feasible
Barlow	II: Extensive prolapse ( $\geq 3$ scallops, posterior commissure)	Localized (annulus)	Moderate	Difficult
Rheumatic	IIIa but pliable anterior leaflet	Localized	Moderate	Difficult
Severe barlow	II: Extensive prolapse ( $\geq 3$ scallops, anterior commissure)	Extensive (annulus+leaflets)	Severe	Unlikely
Endocarditis	II: Prolapse but destructive lesions	No	No/mild	Unlikely
Rheumatic	IIIa but stiff anterior leaflet	Extensive (annulus+leaflets)	Moderate/severe	Unlikely
Secondary	IIIb but severe valvular deformation	No	No or severe	Unlikely

**Table 7** Unfavourable TTE characteristics for mitral valve repair in secondary MR<sup>33</sup>

Mitral valve deformation
Coaptation distance $\geq 1$ cm
Tenting area $> 2.5\text{--}3$ cm <sup>2</sup>
Complex jets originating centrally and posteromedially
Postero-lateral angle $> 45^\circ$ (high posterior leaflet tethering)
Local LV remodelling
Interpapillary muscle distance $> 20$ mm
Posterior papillary-fibrosa distance $> 40$ mm
Lateral wall motion abnormality
Global LV remodelling
EDD $> 65$ mm, ESD $> 51$ mm (ESV $> 140$ mL) (low likelihood of reverse LV remodelling after repair and poor long-term outcome)
Systolic sphericity index $> 0.7$

EDD, end-diastolic diameter; ESD, end-systolic diameter; ESV, end-systolic volume; LV, left ventricle.

appear at the same time narrow in the four-chamber view and broad in the two-chamber view. Moreover, conventional 2D colour Doppler imaging does not provide appropriate orientation of 2D scan planes to obtain an accurate cross-sectional view of the VC. In case of multiple MR jets, the respective widths of the multiple VC are not additive. Such characteristics may be better appreciated and measured by 3D echocardiography. In secondary MR, an average of VC widths (four- and two-chamber views) has been shown to be better correlated with the 3D VC area. An average value  $> 8$  mm on 2D echo (Figure 23) has been reported to define severe MR for all aetiologies of MR including functional MR.<sup>42,43</sup> These data need, however, to be confirmed in further studies.

**Key point: When feasible, the measurement of VC is recommended to quantify MR. Intermediate VC values (3–7 mm) need confirmation by a more quantitative method, when feasible. The VC can often be obtained in eccentric jet. In case of multiple jets, the respective values of the VC width are not additive. The assessment of the VC by 3D echo is still reserved for research purposes.**

*The flow convergence method.* The flow convergence method is the most recommended quantitative approach whenever feasible.<sup>44</sup>

(Figure 24) The apical four-chamber view is classically recommended for optimal visualization of the PISA. However, the parasternal long- or short-axis view is often useful for visualization of the PISA in case of anterior mitral valve prolapse. The area of interest is optimized by lowering imaging depth and reducing the Nyquist limit to  $\sim 15\text{--}40$  cm/s. The radius of the PISA is measured at mid-systole using the first aliasing. R Vol and EROA are obtained using the standard formulas (Figure 25). Qualitatively, the presence of flow convergence at a Nyquist limit of  $50\text{--}60$  cm/s should alert to the presence of severe MR. Grading of the severity of primary MR classifies regurgitation as mild, moderate, or severe, and subclassifies the moderate regurgitation group into 'mild-to-moderate' (EROA of  $20\text{--}29$  mm<sup>2</sup> or an R Vol of  $30\text{--}44$  mL) and 'moderate-to-severe' (EROA of  $30\text{--}39$  mm<sup>2</sup> or an R Vol of  $45\text{--}59$  mL). Quantitatively, primary MR is considered severe if EROA is  $\geq 40$  mm<sup>2</sup> and R Vol  $\geq 60$  mL. In secondary MR, the thresholds of severity, which are of prognostic value, are  $20$  mm<sup>2</sup> and  $30$  mL, respectively.<sup>45</sup> EROA is the most robust parameter as it represents a marker of lesion severity. A large EROA can lead to large regurgitant kinetic energy (large R Vol) but also to potential energy, with low R Vol but high LA pressure.

The PISA method faces several advantages and limitations (Figures 26–29).<sup>2,3,44</sup> The colour M-mode is important to assess the variation of MR flow and the related PISA during systole (Figure 26). The PISA radius is most frequently constant in patients with rheumatic MR. It frequently increases progressively with a maximum during the second half of systole in patients with mitral valve prolapse. In the presence of functional MR, there is a dynamic variation of the regurgitant orifice area with early and late systolic peaks and a mid-systolic decrease. These changes reflect the phasic variation in transmitral pressure that acts to close the mitral leaflets more effectively when pressure reaches its peak in mid-systole.<sup>46</sup> The PISA method is based on the assumption of hemispheric symmetry of the velocity distribution proximal to the circular regurgitant lesion, which may not hold for eccentric jets, multiple jets, or complex or elliptical regurgitant orifices. Practically, the geometry of the PISA varies, depending on the shape of the orifice and mitral valve leaflets surrounding the orifice. In functional MR, the PISA might look like an ellipsoidal shape and two separate MR jets originating from the medial and lateral sides of the coaptation line can be observed on 2D echo. When the shape of the flow convergence zone is not a hemisphere, the PISA method may underestimate the degree of functional MR, particularly when the ratio of long-axis

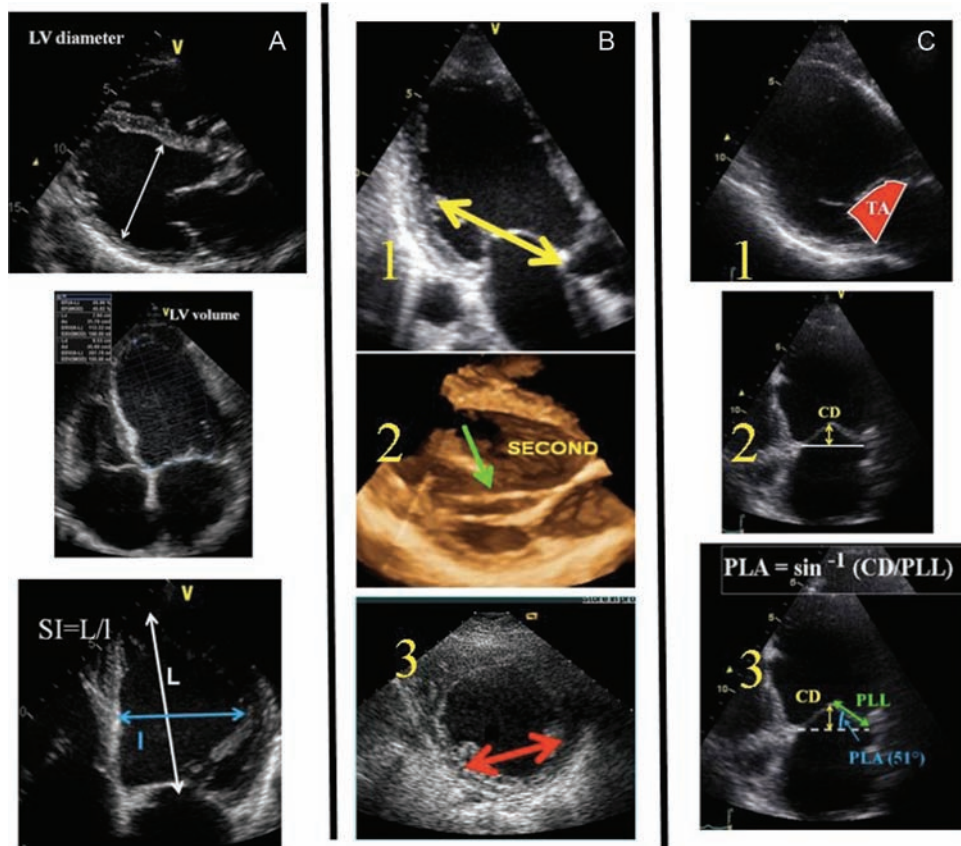


**Figure 20** Echo morphological parameters that are measured in ischaemic MR. (A) global LV remodeling [diameter, LV volumes, sphericity index ( $SI = L/l$ ; L, major axis; l, minor axis)]; (B) local LV remodeling (1: apical displacement of the posteromedial papillary muscle; 2: second order chordate; 3: interpapillary muscle distance); (C) mitral valve deformation [1: systolic tenting area (TA); 2: coaptation distance (CD); 3: postero-lateral angle (PLA)].

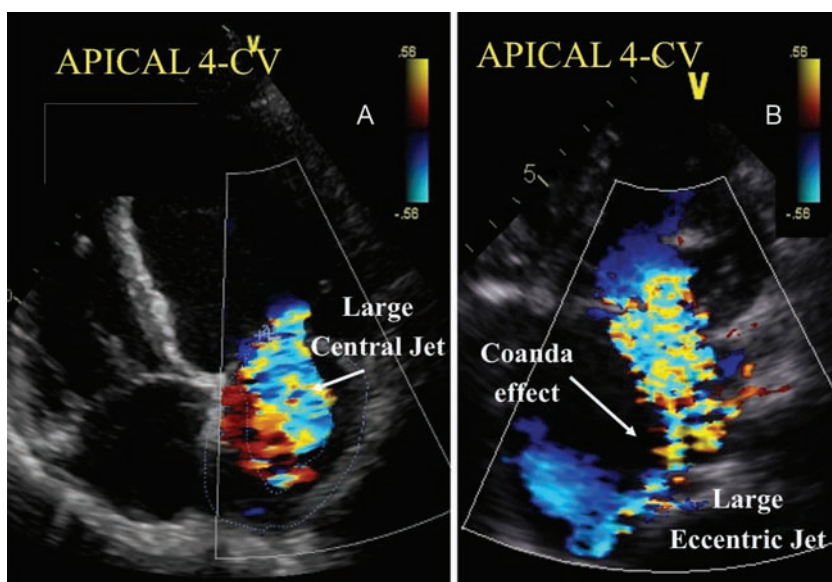


**Figure 21** Visual assessment of mitral regurgitant jet using colour-flow imaging. Examples of two patients with severe mitral regurgitation: (A) large central jet; (B) large eccentric jet with a clear Coanda effect. CV, four-chamber view.

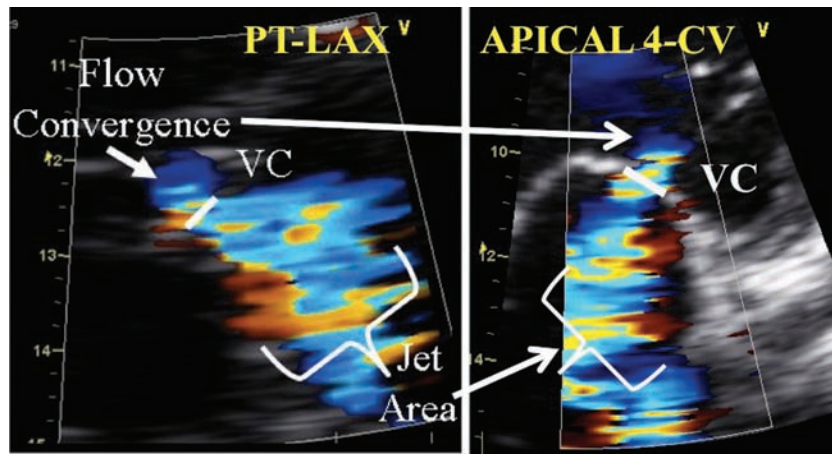


**Figure 22** Semi-quantitative assessment of MR severity using the vena contracta width (VC). The three components of the regurgitant jet (flow convergence zone, vena contracta, jet turbulence) are obtained. CV, chamber view; PT-LAX, parasternal long-axis view.

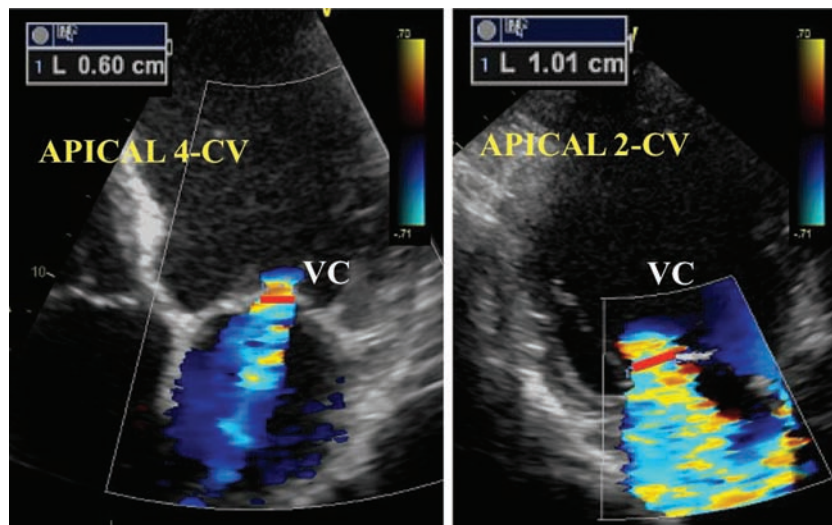


**Figure 23** Semi-quantitative assessment of MR severity using the vena contracta width (VC) obtained from the apical four-chamber and two-chamber views (CV) in a patient with ischaemic functional MR. The mean vena contracta is calculated ( $6 + 10 / 2 = 8$  mm).

length to short-axis length of the 3D regurgitant orifice is  $>1.5$ .<sup>47</sup> When the EROA is calculated with the hemispheric assumption (using the vertical PISA), the horizontal length of PISA is ignored. In organic MR, the shape of the PISA is rounder, which minimizes the risk of EROA underestimation (Figure 29). These findings could explain why the threshold used to define a severe functional MR is inferior to that used for organic MR. Careful consideration of the 3D geometry of PISA may be of interest in evaluating the severity of functional MR. The best 3D echo method to quantitate MR severity remains to be defined.

**Key point: When feasible, the PISA method is highly recommended to quantitate the severity of MR. It can be used in both central and eccentric jets. An EROA**

**$\geq 40 \text{ mm}^2$  or an R Vol  $\geq 60 \text{ mL}$  indicates severe organic MR. In functional ischaemic MR, an EROA  $\geq 20 \text{ mm}^2$  or an R Vol  $\geq 30 \text{ mL}$  identifies a subset of patients at an increased risk of cardiovascular events.**

*Pulsed Doppler*

*Doppler volumetric method.* The quantitative PW Doppler method can be used as an additive or alternative method, especially when the PISA and the VC are not accurate or not applicable. This approach is time-consuming and is associated with several drawbacks.<sup>1–3,48</sup> Briefly, mitral R Vol is obtained by calculating the difference between the total stroke volume (product of the mitral annulus area— $\pi d^2/4 = 0.785 d^2$ , where d is the mitral annulus diameter—

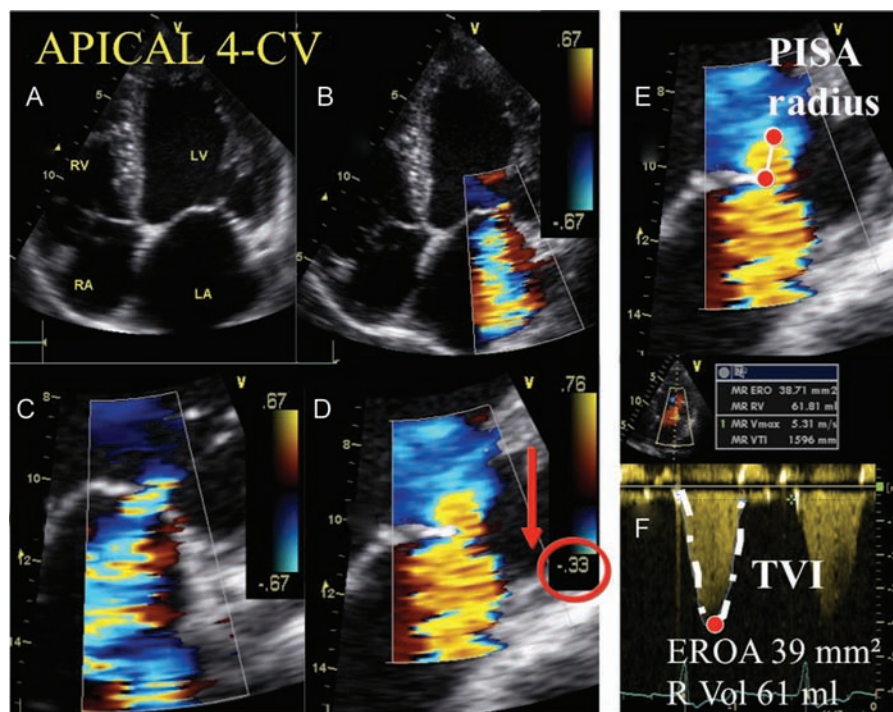


**Figure 24** Quantitative assessment of MR severity using the PISA method. Stepwise analysis of MR: (A) apical four-chamber view (CV); (B) colour-flow display; (C) zoom of the selected zone; (D) downward shift of zero baseline to obtain a hemispheric PISA; (E) measure of the PISA radius using the first aliasing; (F) continuous wave Doppler of MR jet allowing calculation the effective regurgitant orifice area (EROA) and regurgitant volume (R Vol). TVI, time-velocity integral.

and mitral inflow TVI) and systemic stroke volume (obtained by multiplying the LVOT area— $\pi d^2/4 = 0.785 d^2$ , where  $d$  is the LVOT diameter—by LVOT TVI). This calculation is inaccurate in the presence of significant AR.

**Key point: The Doppler volumetric method is a time-consuming approach that is not recommended as a first-line method to quantify MR severity.**

*Anterograde velocity of mitral inflow: mitral to aortic TVI ratio.* In the absence of mitral stenosis, the increase in the transmitral flow that occurs with increasing MR severity can be detected as higher flow velocities during early diastolic filling (increased E velocity). In the absence of mitral stenosis, a peak E velocity  $>1.5$  m/s suggests severe MR. Conversely, a dominant A-wave (atrial contraction) basically excludes severe MR. These patterns are more applicable in patients older than 50 years or in conditions of impaired myocardial relaxation. The pulsed Doppler mitral to aortic TVI ratio is also used as an easily measured index for the quantification of isolated pure organic MR. Mitral inflow Doppler tracings are obtained at the mitral leaflet tips and aortic flow at the annulus level in the apical four-chamber view. A TVI ratio  $>1.4$  strongly suggests severe MR, whereas a TVI ratio  $<1$  is in favour of mild MR (Figure 30).<sup>49</sup>

*Pulmonary venous flow.* The pulsed Doppler evaluation of the pulmonary venous flow pattern is another aid for grading the severity of MR (Figure 30).<sup>50</sup> In normal individuals, a positive systolic wave (S) followed by a smaller diastolic wave (D) is classically seen in the absence of diastolic dysfunction. With increasing the severity of MR, there is a decrease of the S-wave velocity. In severe MR, the

S-wave becomes frankly reversed. As unilateral pulmonary flow reversal can occur at the site of eccentric MR jets if the jet is directed into the sampled vein, sampling through all pulmonary veins is recommended, especially during TOE. Although the evaluation of the right upper pulmonary flow can often be obtained using TTE, evaluation is best performed using TOE with the pulsed Doppler sample placed  $\sim 1$  cm deep into the pulmonary vein. Atrial fibrillation and elevated LA pressure from any cause can blunt forward systolic pulmonary vein flow. Therefore, blunting of pulmonary venous flow lacks of specificity for the diagnosis of severe MR, whereas systolic pulmonary flow reversal is specific for severe MR.

**Key point: Both the pulsed Doppler mitral to aortic TVI ratio and the systolic pulmonary flow reversal are specific for severe MR. They represent the strongest additional parameters for evaluating MR severity.**

#### *Continuous wave Doppler of MR jet*

Peak MR jet velocities by CW Doppler typically range between 4 and 6 m/s. This reflects the high systolic pressure gradient between the LV and LA. The velocity itself does not provide useful information about the severity of MR. Conversely, the signal intensity (jet density) of the CW envelope of the MR jet can be a qualitative guide to MR severity. A dense MR signal with a full envelope indicates more severe MR than a faint signal (Figure 30). The CW Doppler envelope may be truncated (notched) with a triangular contour and an early peak velocity (blunt). This indicates elevated LA pressure or a prominent regurgitant pressure wave in the LA due to severe MR. In eccentric MR, it may be

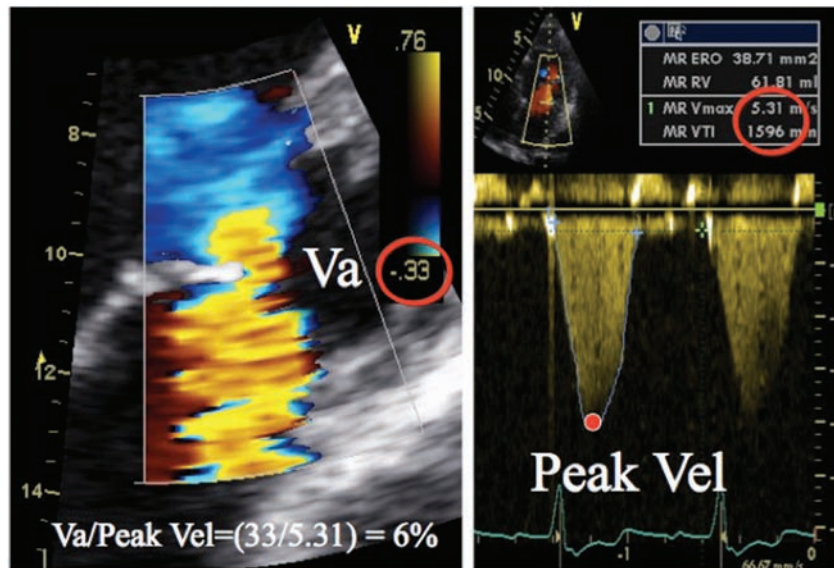


**Figure 25** Quantification of MR using the PISA method. To avoid the underestimation of the regurgitant volume, the ratio of the aliasing velocity (Va) to peak orifice velocity (vel) is maintained < 10%.

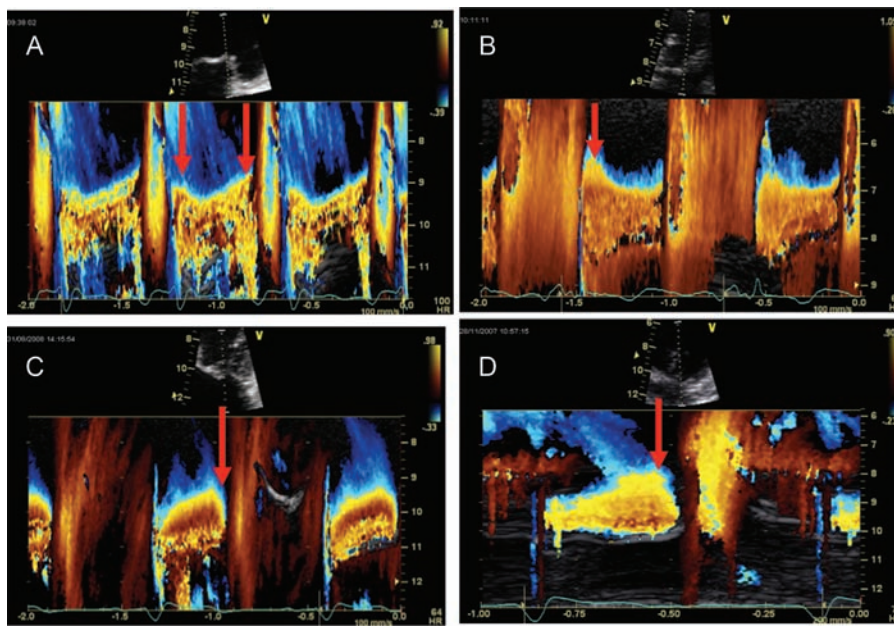


**Figure 26** Four examples of flow convergence zone changes during systole using the colour M-Mode. (A and B) Functional MR [(A) early and late peaks and mid-systolic decreases; (B) early systolic peak], (C) rheumatic MR with an end-systolic decrease in the flow convergence zone, (D) M mitral valve prolapse (late systolic enhancement).

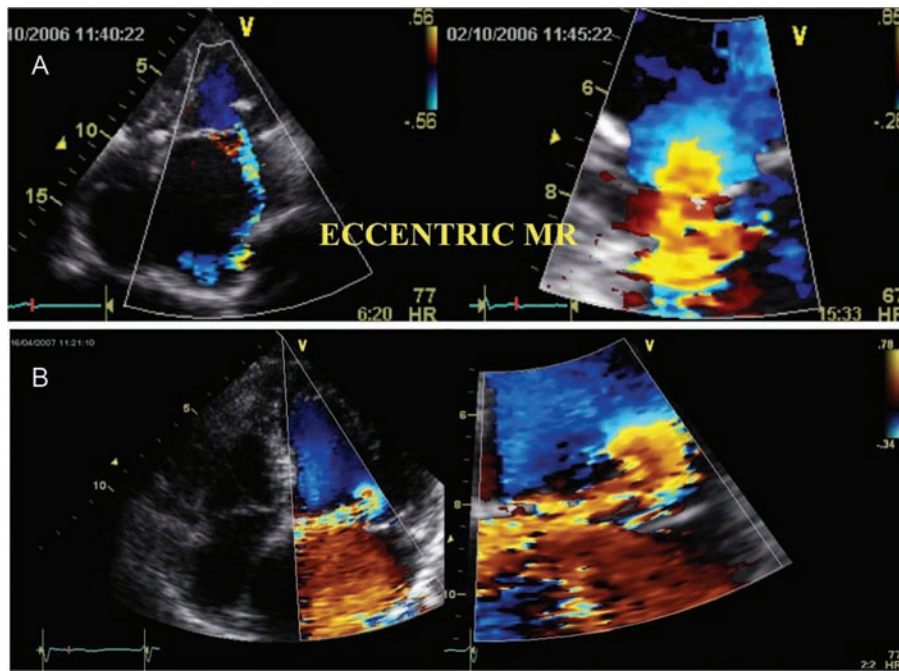


**Figure 27** Examples of eccentric MR that can still be perfectly assessed by using the PISA method.

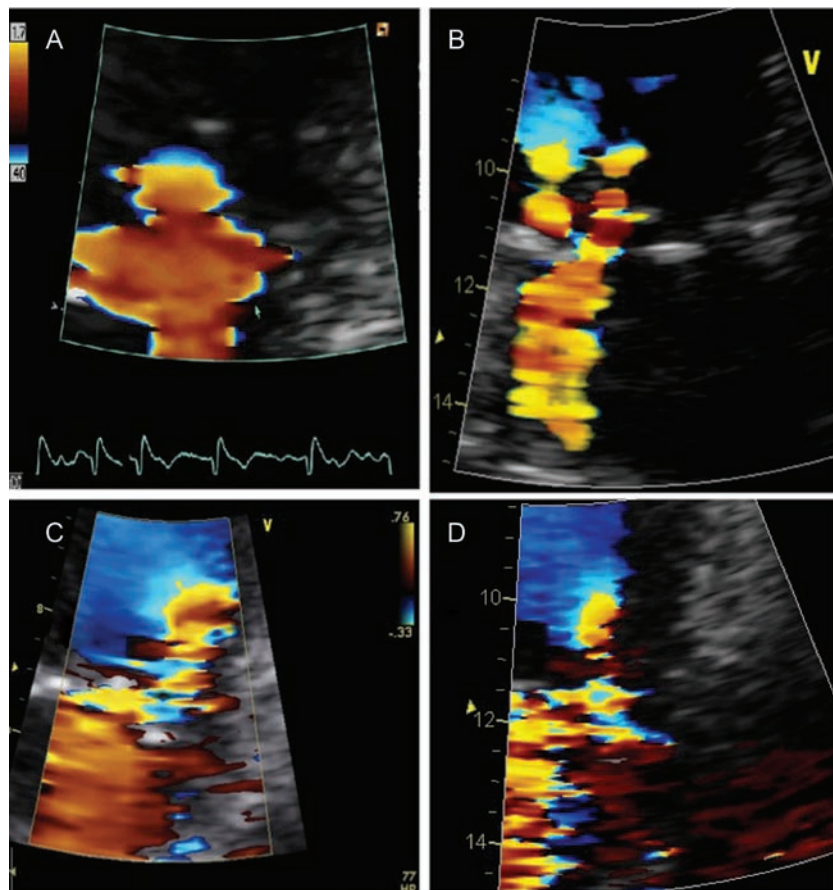


**Figure 28** (A) Example of a flat flow convergence zone; (B) presence of two jets; (C and D) distorted and constrained flow convergence zone by the lateral myocardial wall.



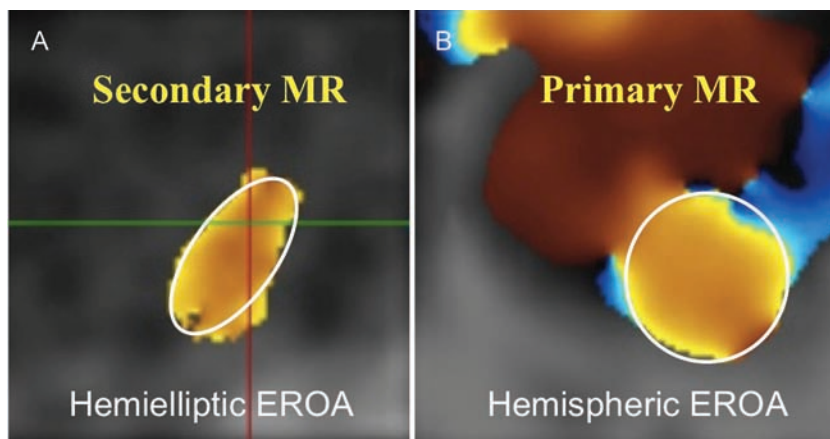


**Figure 29** Three-dimensional shape of the flow convergence in functional (A) (hemielliptic) and organic MR (B) (hemispheric).

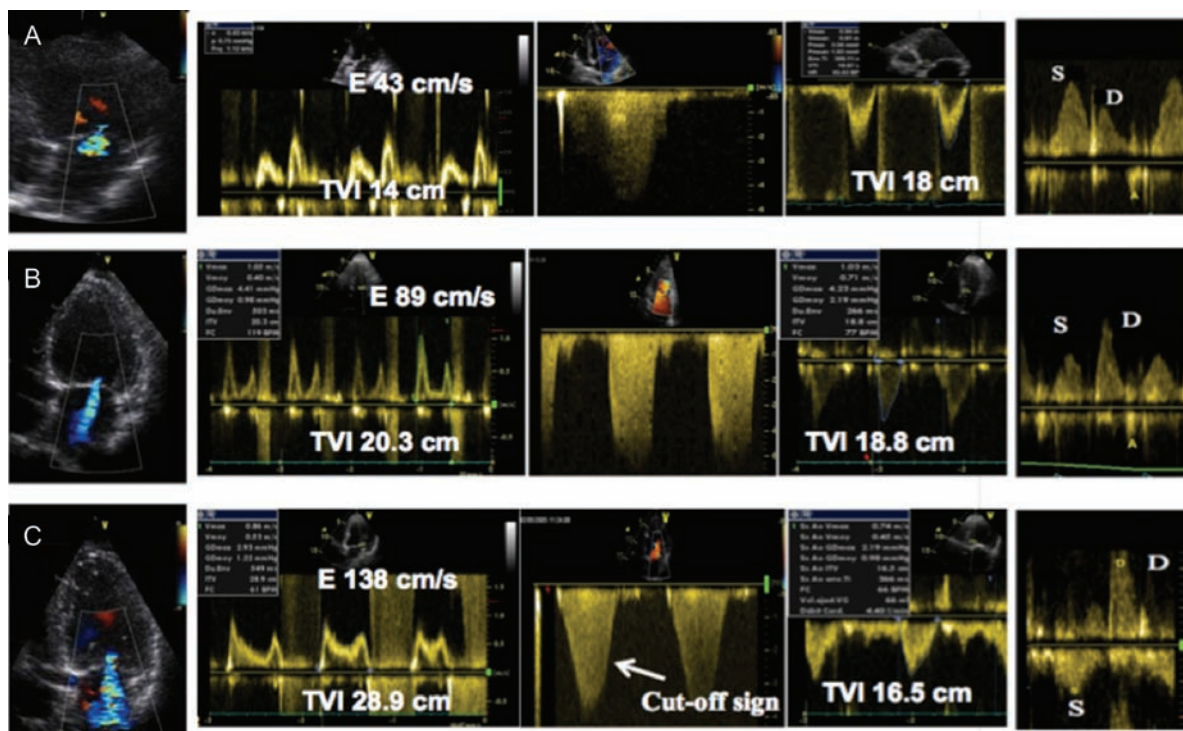


**Figure 30** Three examples of various degrees of MR, mild (A), moderate (B), and severe (C) are provided. The regurgitant jet area (RJA) as well as the mitral E wave velocity increase with the severity of MR. In severe MR, the continuous wave Doppler signal of the regurgitant jet is truncated, triangular, and intense. Notching of the continuous wave envelope (cut-off sign) can occur in severe MR. TVI, time-velocity integral. Mild MR, normal pulmonary vein flow pattern; moderate MR, blunt forward systolic pulmonary vein flow in a patient with moderate MR; severe MR, reversed systolic pulmonary flow in a patient with severe MR. S, systolic wave; (D) diastolic wave.

difficult to record the full-CW envelope of the jet because of its eccentricity, whereas the signal intensity shows dense features.

**Key point: The CW Doppler density of the MR jet is a qualitative parameter of MR severity.**

**Consequences of MR**

The presence of severe primary MR has significant haemodynamic effects, primarily on the LV and LA. In acute primary MR, the LV is classically not enlarged while the LV ejection fraction usually increases in

response to the increased preload. In the chronic compensated phase (the patient could be asymptomatic), the forward stroke volume is maintained through an increase in LV ejection fraction. Such patients typically have LV ejection fraction >65%. In this phase, the LA remodels and dilates but the LA pressure is often normal. In the chronic decompensated phase (the patient could still be asymptomatic or may fail to recognize deterioration in clinical status), the forward stroke volume decreases and the LA pressure increases significantly. The LV contractility can thus decrease silently and irreversibly. However, the LV ejection fraction may still be in the low normal range despite the presence of significant myocardial dysfunction. Hence, dilatation is sensitive for chronic significant MR, whereas normal size almost excludes severe chronic MR. However, dilatation can be observed in other conditions or may be absent in acute severe MR and is, therefore, a non-specific finding. Of note, the excess regurgitant blood entering the LA may induce a progressive rise in pulmonary arterial pressure and a significant tricuspid annular dilatation. Secondary MR has a different physiology, as it is the consequence of an initial ventricular disease. The LV and LA dilatation are in excess to the degree of MR. The LA pressure is often elevated despite lower regurgitant volume than in primary MR.

**Key point: When MR is more than mild MR, providing the LV diameters, volumes, and ejection fraction as well as the LA dimensions (preferably LA volume) and the pulmonary arterial systolic pressure in the final echocardiographic**

**report is mandatory.<sup>1</sup> The quantitative assessment of myocardial function (systolic myocardial velocities, strain, strain rate) is reasonable, particularly in asymptomatic patients with severe primary MR and borderline values in terms of LV ejection fraction (60–65%) or LV end-systolic diameter (close to 40 mm or 22 mm/m<sup>2</sup>).**

### Integrating indices of severity

The echocardiographic assessment of MR includes integration of data from 2D/3D imaging of the valve and ventricle as well as Doppler measures of regurgitation severity (Table 8). Effort should be made to quantify the degree of regurgitation, except in the presence of mild or obviously severe MR. Both the VC width and the PISA method are recommended. Adjunctive parameters help to consolidate about the severity of MR and should be widely used particularly when there is discordance between the quantified degree of MR and the clinical context. For instance, a modest regurgitant volume reflects severe MR when it develops acutely into a small, non-compliant LA and it may cause pulmonary congestion and systemic hypotension.

## TR

TR is a common finding. Since it is mostly asymptomatic and not easily audible on physical examination, it is frequently only diagnosed by echocardiography performed for other indications. Although a

**Table 8 Grading the severity of primary MR**

Parameters	Mild	Moderate	Severe
Qualitative			
MV morphology	Normal/abnormal	Normal/abnormal	Flail leaflet/ruptured PMs
Colour flow MR jet	Small, central	Intermediate	Very large central jet or eccentric jet adhering, swirling and reaching the posterior wall of the LA
Flow convergence zone <sup>a</sup>	No or small	Intermediate	Large
CW signal of MR jet	Faint/parabolic	Dense/parabolic	Dense/triangular
Semi-quantitative			
VC width (mm)	<3	Intermediate	≥7 (>8 for biplane) <sup>b</sup>
Pulmonary vein flow	Systolic dominance	Systolic blunting	Systolic flow reversal <sup>c</sup>
Mitral inflow	A wave dominant <sup>d</sup>	Variable	E-wave dominant (>1.5 m/s) <sup>e</sup>
TVI mit /TVI Ao	<1	Intermediate	>1.4
Quantitative			
EROA (mm <sup>2</sup> )	<20	20–29; 30–39 <sup>g</sup>	≥40
R Vol (mL)	<30	30–44; 45–59 <sup>g</sup>	≥60
+ LV and LA size and the systolic pulmonary arterial pressure <sup>f</sup>			

CW, continuous wave; LA, left atrium; EROA, effective regurgitant orifice area; LV, left ventricle; MR, mitral regurgitation; R Vol, regurgitant volume; VC, vena contracta.

<sup>a</sup>At a Nyquist limit of 50–60 cm/s.

<sup>b</sup>For average between apical four- and two-chamber views.

<sup>c</sup>Unless other reasons of systolic blunting (atrial fibrillation, elevated LA pressure).

<sup>d</sup>Usually after 50 years of age.

<sup>e</sup>In the absence of other causes of elevated LA pressure and of mitral stenosis.

<sup>f</sup>Unless for other reasons, the LA and LV size and the pulmonary pressure are usually normal in patients with mild MR. In acute severe MR, the pulmonary pressures are usually elevated while the LV size is still often normal. In chronic severe MR, the LV is classically dilated. Accepted cut-off values for non-significant left-sided chambers enlargement: LA volume <36 mL/m<sup>2</sup>, LV end-diastolic diameter <56 mm, LV end-diastolic volume <82 mL/m<sup>2</sup>, LV end-systolic diameter <40 mm, LV end-systolic volume <30 mL/m<sup>2</sup>, LA diameter <39 mm, LA volume <29 mL/m<sup>2</sup>.

<sup>g</sup>Grading of severity of organic MR classifies regurgitation as mild, moderate, or severe, and subclassifies the moderate regurgitation group into 'mild-to-moderate' (EROA of 20 to 29 mm<sup>2</sup> or a R Vol of 30 to 44 mL) and 'moderate-to-severe' (EROA of 30–39 mm<sup>2</sup> or a R Vol of 45–59 mL).

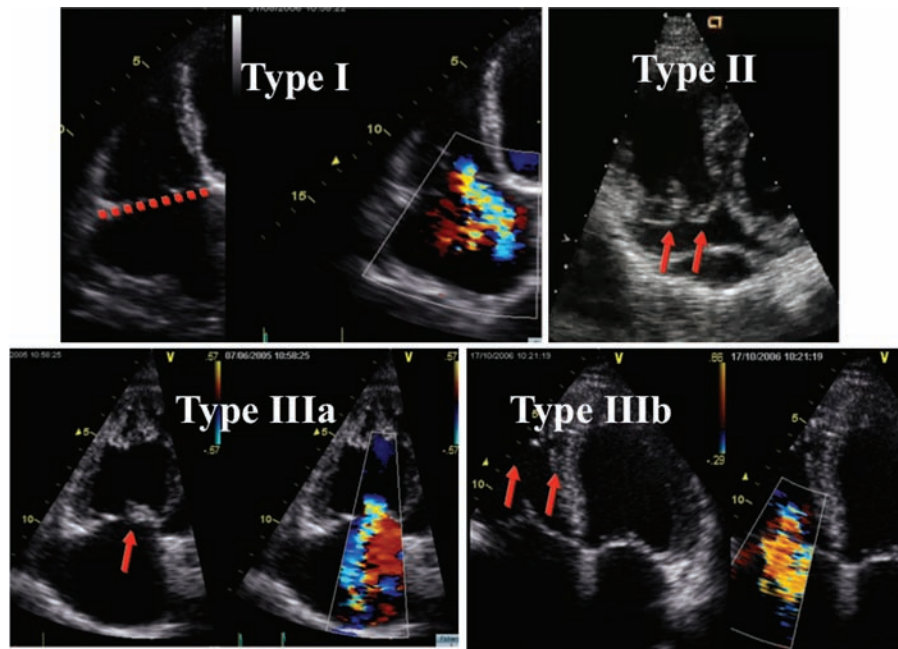


**Figure 31** Mechanisms of MR according to the Carpentier's functional classification.

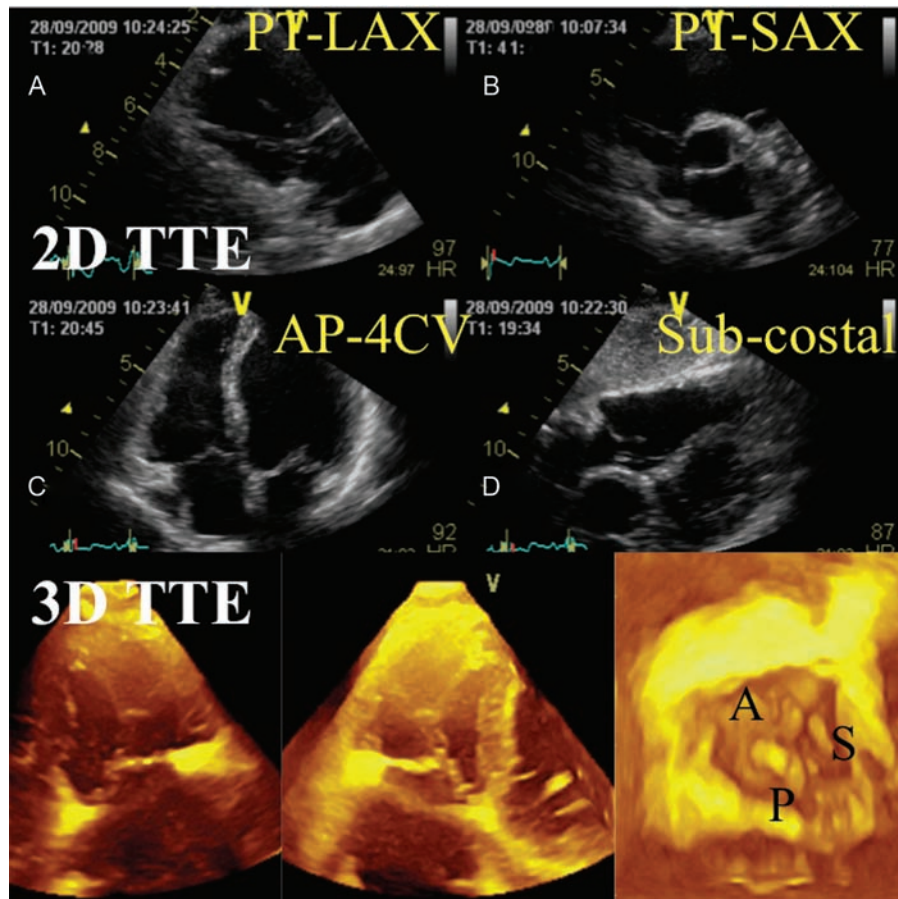


**Figure 32** Two-dimensional and 3D echo recordings of the tricuspid valve. (A) Parasternal long-axis view; (B) parasternal short-axis view at the level of the aortic valve; (C) apical four-chamber view; (D) subcostal view. A, anterior leaflet; S, septal leaflet; P, posterior leaflet.

mild degree of TR is frequent and benign, moderate, and severe TR are associated with poor prognosis.

## Anatomy and function of the tricuspid valve

The tricuspid valve complex is similar to the mitral valve but has greater variability. It consists of the annulus, leaflets, RV, papillary muscles, and chordae tendinae. The tricuspid valve is located between the right atrium (RA) and the RV and is placed in a slightly more apical position than the mitral valve.<sup>51</sup> The tricuspid valve has three leaflets of unequal size: the anterior leaflet is usually the largest and extends from the infundibular region anteriorly to the inferolateral wall posteriorly; the septal leaflet extends from the interventricular septum to the posterior ventricular border; the posterior leaflet attaches along the posterior margin of the annulus from the septum to the inferolateral wall. The insertion of the septal leaflet of the tricuspid valve is characteristically apical relative to the septal insertion of the anterior mitral leaflet.

## Aetiology and mechanisms

The most common cause of TR is not a primary tricuspid valve disease (organic TR) but rather an impaired valve coaptation (secondary or functional TR) caused by dilation of the RV and/or of the tricuspid annulus due to left-sided heart valve diseases, pulmonary hypertension, congenital heart defects, and cardiomyopathy.<sup>52</sup>

The progressive remodelling of the RV cavity leads to tricuspid annular dilatation, papillary muscle displacement and tethering of

the leaflets, resulting in secondary TR. As for secondary MR, secondary TR begets TR. Indeed, TR itself leads to further RV dilation and dysfunction, right atrial enlargement, more tricuspid annular dilatation and tethering, and worsening TR. With increasing TR, the RV dilates and eventually fails, causing increased RV diastolic pressure and, in advanced situation a shift of the interventricular septum towards the LV. Such ventricular interdependence might reduce the LV cavity size (pure compression), causing restricted LV filling and increased LV diastolic and pulmonary artery pressure. The tricuspid annular dilatation, the loss of its contraction and the increased tethering are probably the most important factors in the development of TR. Indeed, the tricuspid annulus is not saddle shaped anymore; it becomes flat, planar and distorted.<sup>52,53</sup>

A variety of primary disease processes can affect the tricuspid valve complex directly and lead to valve incompetence: infective endocarditis, congenital disease like Ebstein anomaly or atrioventricular canal, rheumatic fever (commissural fusion, shortening and retraction of one or more leaflets and of the chordae tendinae), carcinoid syndrome (lack of commissural fusion, thickened valve with markedly restricted motion during cardiac cycle), endomyocardial fibrosis, myxomatous degeneration of the tricuspid valve leading to prolapse or flail tricuspid valve, penetrating and non-penetrating trauma, and iatrogenic damages during cardiac surgery, biopsies, and catheter placement in right heart chambers.<sup>54</sup>

The Carpentier's classification remains the most common used functional classification in TR: type I: leaflet perforation (infective endocarditis) or more frequently by annular dilatation; type II:

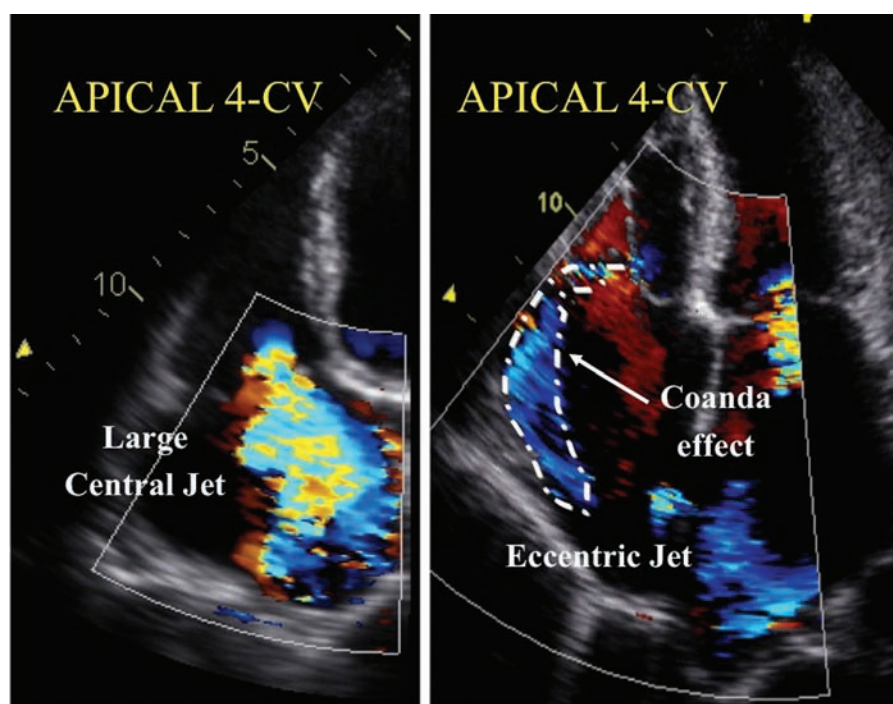


**Figure 33** Visual assessment of tricuspid regurgitant jet using colour-flow imaging. (A) Large central jet; (B) eccentric jet with a clear Coanda effect. CV, four-chamber view.

prolapse of one or more leaflets (tricuspid valve prolapse); and type III: restricted motion as the consequence of rheumatic disease, significant calcifications, toxic valvulopathy, functional TR (Figure 31).

## Echocardiographic evaluation in TR

### Tricuspid valve morphology

The three main TTE views allowing the tricuspid valve visualization are the parasternal (long-axis view of RV inflow, short-axis view at the level of the aortic valve), the apical 4-chamber and the subcostal views. TOE for the tricuspid valve is possible with the 4-chamber view at 0 degree in the basal transoesophageal and oesogastric junction planes. TOE is of interest for the diagnosis of endocarditis, venous catheters and pacemakers lead infection, and visualization of traumatic rupture of the tricuspid valve. However, it is rarely possible to visualize by 2D echo the three leaflets simultaneously (usually from a modified subcostal view). Therefore, the designation of individual leaflets of the tricuspid valve should be done with caution unless a simultaneous view of all three cusps is obtained. Real-time 3D TTE is more routinely available and allows, with its unique capability of obtaining a short-axis plane of the tricuspid valve, simultaneous visualization of the three leaflets moving during the cardiac cycle, their commissures and their attachment to the tricuspid annulus.<sup>52–54</sup> (Figure 32)

In the pathologic TR, a complete understanding of leaflet morphology and of the pathophysiological mechanisms underlying TR could potentially lead to improved techniques for valve repair and to design physiologically suitable annular rings. It should be stressed that TR is most often seen in patients with multiple valvular disease especially aortic or mitral valve disease. In secondary TR, increased tethering (apical displacement of the tricuspid leaflets) can be evaluated by the measurement of the systolic tenting area (area between the tricuspid annulus and the tricuspid leaflets body) and the coaptation distance (distance between the tricuspid annular plane and the point of coaptation) in mid-systole from the apical 4-chamber view. A tenting area  $> 1 \text{ cm}^2$  has been shown to be associated with severe TR.<sup>55</sup> The tricuspid annulus shows a non-planar structure with an elliptical saddle-shaped pattern, having two high points (oriented superiorly towards the RA) and two low points (oriented inferiorly towards the RV that is best seen in mid-systole).<sup>56</sup> Normal tricuspid valve annulus diameter in adults is  $28 \pm 5 \text{ mm}$  in the four-chamber view. Significant tricuspid annular dilatation is defined by a diastolic diameter of  $> 21 \text{ mm/m}^2$  ( $> 35 \text{ mm}$ ). The normal contraction (decrease in the annular area in systole) of the tricuspid annulus is 25%.

### Predictors of successful valve repair

Persistent or recurrent TR has been reported in up to 20–50% of patients undergoing mitral valve surgery.<sup>57</sup> In secondary TR, this has been related to the extent of tricuspid leaflet restriction and to the severity of tricuspid annular dilatation.<sup>52</sup> Both the severity of pre-operative TR and RV dysfunction contributes to residual post-operative TR. Similarly, severe tricuspid valve tethering predicts residual TR after tricuspid valve annuloplasty. A tenting area  $> 1.63 \text{ cm}^2$  and a tethering distance  $> 0.76 \text{ cm}$  are good predictors of residual TR after tricuspid valve surgery.<sup>58</sup>

### Assessment of TR severity

#### Colour flow Doppler

Grading the severity of TR is in principle similar to MR. However, because standards for determining the TR severity are less robust than for MR, the algorithms for relating colour flow-derived parameters to TR severity are less well developed.

**Colour flow imaging.** Colour-flow imaging is useful to recognize small jets, but the assessment of larger TR jets has important limitations.<sup>59</sup> Indeed, flow jets that are directed centrally into the RA generally appear larger than eccentric wall-impinging jets with similar or worse severity. Basically, multiple windows (apical four-chamber, parasternal long- and short-axis views, subcostal view) are recommended to assess TR severity by colour-flow analysis. The general assumption is that larger colour jets that extend deep into the RA represent more TR than smaller thin jets that are seen just beyond the tricuspid leaflets. As for MR, this method is a source of many errors and is limited by several technical and haemodynamic factors. Furthermore, colour flow imaging is not recommended for assessing TR severity (Figure 33). Nevertheless, the detection of a large eccentric jet adhering, swirling, and reaching the posterior wall of the RA is in favour of severe TR. Conversely, small thin central jets usually indicate mild TR.

**Key point: The colour flow area of the regurgitant jet is not recommended to quantify the severity of TR. The**

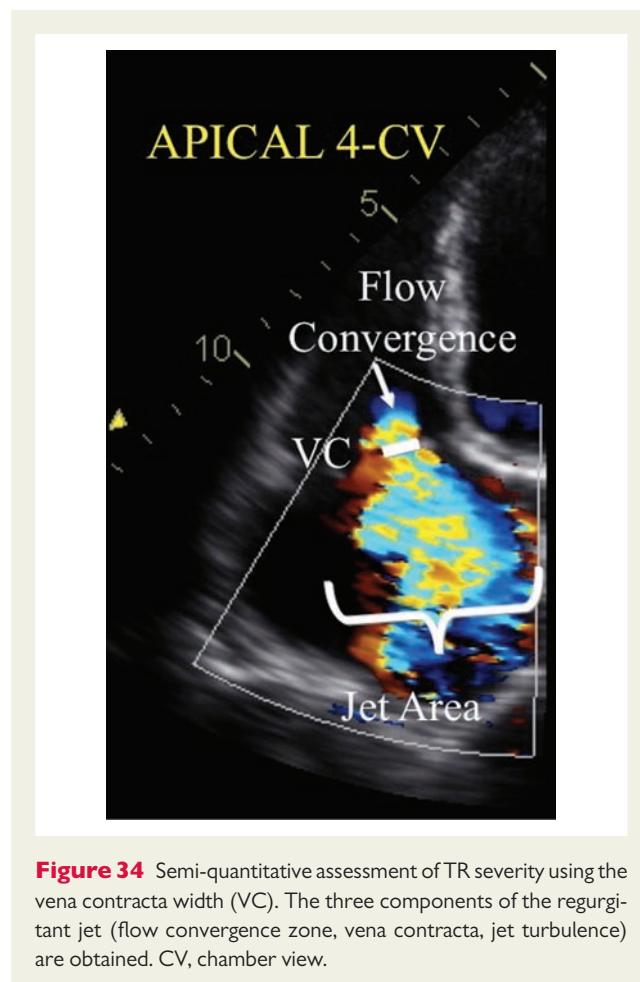


**Figure 34** Semi-quantitative assessment of TR severity using the vena contracta width (VC). The three components of the regurgitant jet (flow convergence zone, vena contracta, jet turbulence) are obtained. CV, chamber view.

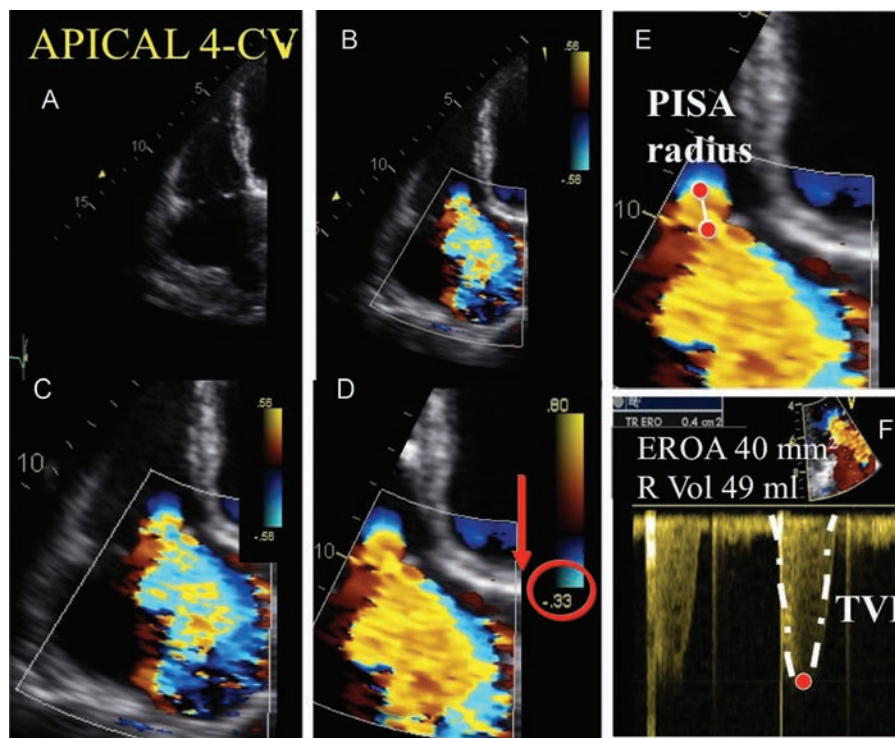


**Figure 35** Quantitative assessment of TR severity using the PISA method. Stepwise analysis of MR: (A) apical four-chamber view (CV); (B) colour-flow display; (C) zoom of the selected zone; (D) downward shift of zero baseline to obtain a hemispheric PISA; (E) measure of the PISA radius using the first aliasing; (F) continuous wave Doppler of TR jet allowing calculation the effective regurgitant orifice area (EROA), and regurgitant volume (R Vol). TVI, time-velocity integral.

**colour flow imaging should only be used for diagnosing TR. A more quantitative approach is required when more than a small central TR jet is observed.**

**VC width.** The VC width of the TR is typically imaged in the apical four-chamber view using the same settings as for MR (Figure 34). Averaging measurements over at least two to three beats is recommended. A VC  $\geq 7$  mm is in favour of severe, whereas a diameter  $< 6$  mm may be either mild or moderate TR.<sup>60</sup> The geometry of the regurgitant orifice of secondary TR is usually more complex than the one of MR and not necessarily circular.<sup>52</sup> A poor correlation has been suggested between the 2D VC width and the 3D assessment of the EROA. This could underline the poor accuracy of the 2D VC width in eccentric jets. With 3D echo, an EROA  $> 75$  mm<sup>2</sup> seems to indicate severe TR.<sup>61</sup> However, these data need to be confirmed in further studies.

**Key point: When feasible, the measurement of the VC is recommended to quantify TR. A VC width  $\geq 7$  mm defines severe TR. Lower values are difficult to interpret. In case of multiple jets, the respective values of the VC width are not additive. The assessment of the VC by 3D echo is still reserved to research purposes.**

**The flow convergence method.** Although providing quantitative assessment, clinical practice reveals that the flow convergence method is rarely applied in TR (Figure 35) also because one of the basic assumptions (circularity of regurgitant orifice) for its application is rarely met in secondary TR. This approach has been validated in small

studies.<sup>62–64</sup> The apical four-chamber view and the parasternal long- and short-axis views are classically recommended for optimal visualization of the PISA. The area of interest is optimized by lowering imaging depth and the Nyquist limit to  $\sim 15$ – $40$  cm/s. The radius of the PISA is measured at mid-systole using the first aliasing (Figure 30). Qualitatively, a TR PISA radius  $\geq 9$  mm at a Nyquist limit of 28 cm/s alerts to the presence of severe TR, whereas a radius  $< 5$  mm suggests mild TR.<sup>63</sup> An EROA  $\geq 40$  mm<sup>2</sup> or an R Vol of  $\geq 45$  mL indicates severe TR. The PISA method faces several advantages and limitations.<sup>1–3</sup> It could underestimate the severity of TR by up to 30%. This method is also less accurate in eccentric jets. To note, the number of studies having evaluated the value of the flow convergence method in TR are still limited.

**Key point: When feasible, the measurement of the PISA radius is reasonable to quantify the TR severity. A TR PISA radius  $> 9$  mm at a Nyquist limit of 28 cm/s indicates severe TR.**

#### Pulsed Doppler

**Doppler volumetric method.** The quantitative PW Doppler method has not been validated to quantify the TR severity. This approach is not recommended.

**Anterograde velocity of tricuspid inflow.** Similar to MR, the severity of TR will affect the early tricuspid diastolic filling (E velocity). In the absence of tricuspid stenosis, the peak E velocity increases in proportion to the degree of TR. Tricuspid inflow Doppler tracings are obtained at the tricuspid leaflet tips. A peak E velocity  $> 1$  m/s suggests severe TR (Figure 36).

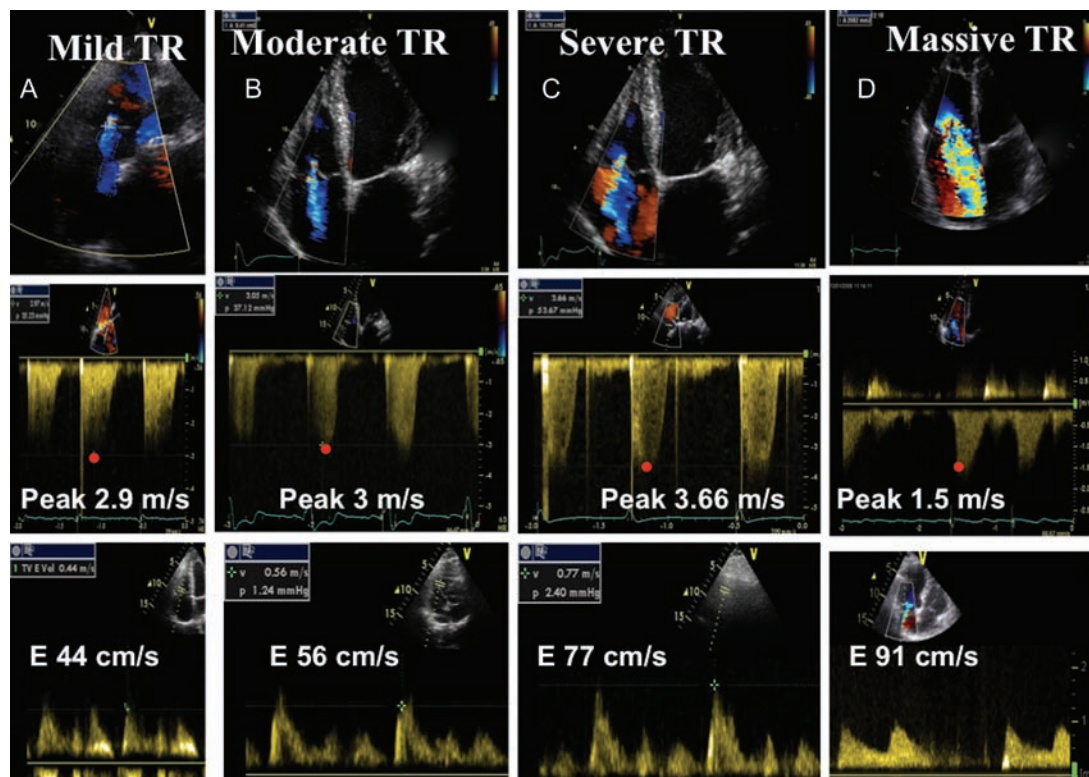


**Figure 36** Four examples of various degrees of TR, mild (A), moderate (B), severe (C), and massive (D) are provided. The regurgitant jet area (RJA) as well as the tricuspid E-wave velocity increase with the severity of TR. In severe TR, the continuous wave Doppler signal of the regurgitant jet is truncated, triangular, and intense. The peak velocity of TR (continuous wave Doppler) allows the estimation of pulmonary pressure except in case of massive TR, since the Bernoulli equation is not applicable.

**Hepatic vein flow.** The pulsed Doppler evaluation of the hepatic venous flow pattern is another aid for grading TR. In normal individuals, the pattern of flow velocity consists of anterograde systolic, transient flow reversal as the TV annulus recoils at the end of systole, anterograde diastolic, and a retrograde A-wave caused by atrial contraction. Such hepatic flow patterns are affected by respiration. With increasing the severity of TR, there is a decrease in hepatic vein systolic velocity. In severe TR, systolic flow reversal occurs (Figure 37). The sensitivity of flow reversal for severe TR is 80%.<sup>59</sup> Thus, the absence of systolic flow reversal does not rule out severe TR. Blunted systolic hepatic vein flow can be observed in case of abnormal right atrial and RV compliance, atrial fibrillation, and elevated right atrial pressure from any cause.<sup>65</sup> Blunting of hepatic flow may thus lack of specificity. Retrograde systolic flow can also be seen with colour flow Doppler. It can be associated with phasic spontaneous appearance of some contrast in the hepatic vein.

**Key point: The systolic hepatic flow reversal is specific for severe TR. It represents the strongest additional parameter for evaluating the severity of TR.**

#### Continuous wave Doppler of TR jet

As for MR, the CW envelope of the TR jet can be a guide to TR severity. A dense TR signal with a full envelope indicates more severe TR than a faint signal. The CW Doppler envelope may be truncated (notched) with a triangular contour and an early peak velocity (blunt), which is indicative of elevated right atrial pressure or a prominent

regurgitant pressure wave in the RA due to severe TR. Marked respiratory variation (decreased TR velocity with inspiration) suggests an elevated RA pressure (Kussmaul's sign on physical examination). The TR jet can be used to determine RV or pulmonary artery systolic pressure. This is done by calculating the RV to RA pressure gradient using the modified Bernoulli equation and then adding an assumed RA pressure. To note, the velocity of the TR jet by itself does not provide useful information about the severity of TR. For instance, massive TR is often associated with a low jet velocity (<2 m/s) as there is near equalization of RV and RA pressures.<sup>66</sup> In some case, a high-velocity jet that represents only mild TR may be present when severe pulmonary hypertension is present.

#### Consequences of TR

Signs of severe TR include RA and RV dilatation, a dilated and pulsatile inferior vena cava and hepatic vein, a dilated coronary sinus, and systolic bowing of the interatrial septum towards the LA. An end-systolic RV eccentricity index >2—obtained by dividing the longest right lateral distance by the distance connecting the ventricular septum and the RV free wall—is in favour of severe TR (sensitivity of 79%).<sup>55</sup> Conversely, a poor correlation between the RV area, the fractional area change and the degree of TR has been reported. Moreover, evidence of right heart dilatation is not specific for TR but can be noted in other conditions (pulmonary valve regurgitation,

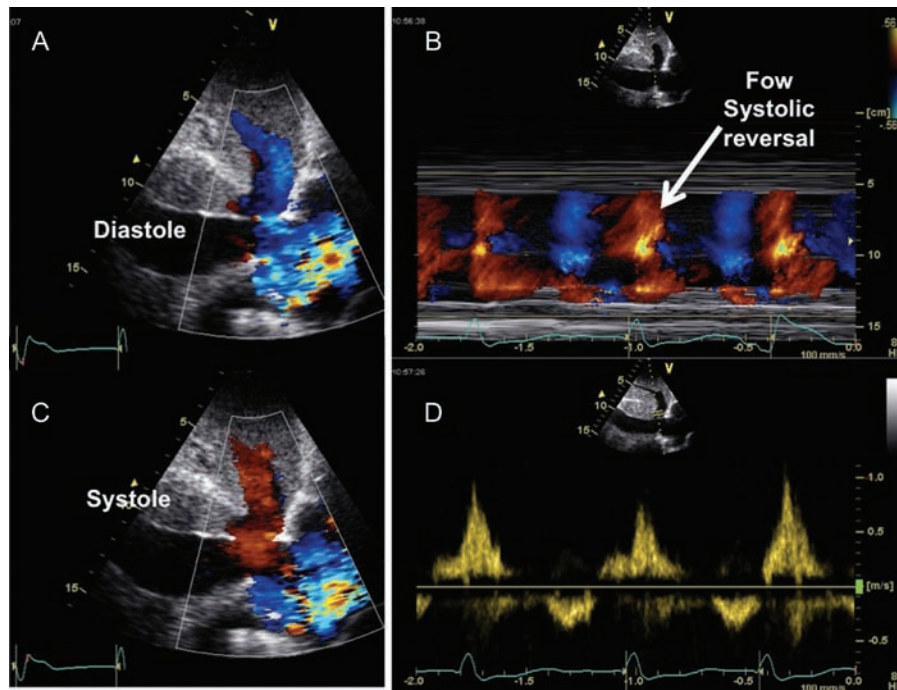


**Figure 37** Subcostal echocardiogram recorded in a patient with severe TR. (A–C) The colour Doppler confirms retrograde flow into the vena cava and hepatic vein in systole consistent with TR (red); (D) A spectral Doppler recording from a hepatic vein, also confirming the systolic retrograde flow.

**Table 9** Grading the severity of TR

Parameters	Mild	Moderate	Severe
<b>Qualitative</b>			
Tricuspid valve morphology	Normal/abnormal	Normal/abnormal	Abnormal/flail/large coaptation defect
Colour flow TR jet <sup>a</sup>	Small, central	Intermediate	Very large central jet or eccentric wall-impinging jet
CW signal of TR jet	Faint/parabolic	Dense/parabolic	Dense/triangular with early peaking (peak < 2 m/s in massive TR)
<b>Semi-quantitative</b>			
VC width (mm) <sup>a</sup>	Not defined	<7	>7
PISA radius (mm) <sup>b</sup>	≤5	6–9	>9
Hepatic vein flow <sup>c</sup>	Systolic dominance	Systolic blunting	Systolic flow reversal
Tricuspid inflow	Normal	Normal	E-wave dominant (≥1 m/s) <sup>d</sup>
<b>Quantitative</b>			
EROA (mm <sup>2</sup> )	Not defined	Not defined	≥40
R Vol (mL)	Not defined	Not defined	≥45
+ RA/RV/IVC dimension <sup>e</sup>			

CW, continuous wave; EROA, effective regurgitant orifice area; RA, right atrium; RV, right ventricle; R Vol, regurgitant volume; TR, tricuspid regurgitation; VC, vena contracta.

<sup>a</sup>At a Nyquist limit of 50–60 cm/s.

<sup>b</sup>Baseline Nyquist limit shift of 28 cm/s.

<sup>c</sup>Unless other reasons of systolic blunting (atrial fibrillation, elevated RA pressure).

<sup>d</sup>In the absence of other causes of elevated RA pressure.

<sup>e</sup>Unless for other reasons, the RA and RV size and IVC are usually normal in patients with mild TR. An end-systolic RV eccentricity index > 2 is in favour of severe TR. In acute severe TR, the RV size is often normal. In chronic severe TR, the RV is classically dilated. *Accepted cut-off values for non-significant right-sided chambers enlargement (measurements obtained from the apical four-chamber view):* Mid-RV dimension ≤ 33 mm, RV end-diastolic area ≤ 28 cm<sup>2</sup>, RV end-systolic area ≤ 16 cm<sup>2</sup>, RV fractional area change > 32%, maximal 2D RA volume ≤ 33 mL/m<sup>2</sup>.

An IVC diameter < 2.1 cm is considered normal.



left-to-right atrial shunt, anomalous venous return). However, its absence suggests milder degree of TR. RV dysfunction may be seen in both left-sided and right-sided valvular heart disease. In unoperated patients with mitral valve disease, subnormal RV ejection fraction at rest is associated with decreased exercise tolerance and mortality. In operated patients, an RV ejection fraction <20% predicted post-operative death.<sup>67</sup> Progressive RV dysfunction may also result from chronic TR. In a recent study, it has been shown that flail tricuspid valve is associated with decreased survival and increasing risk of heart failure.<sup>68</sup> This indicates that sustained severe TR for a long time could lead to significant RV dysfunction. As for the LV, the RV ejection fraction is a crude estimate of RV function. It is dependent on loading conditions, ventricular interaction as well as myocardial structure. Other parameters (tricuspid annular plane systolic excursion or TAPSE, systolic myocardial velocities) are currently available for a better assessment of RV function but they still need to be validated in both left- and right-sided valve diseases. Both the TAPSE and the systolic velocity seem to be, however, less accurate in patients with severe TR,<sup>69</sup> and less load-dependent parameters (i.e. 2D longitudinal strain and strain rate) could be more useful in this setting. Imaging the vena cava and its respiratory variation also provide an evaluation of RA pressure. Although not specific, a rapid anterior motion of the interventricular septum at the onset of systole (isovolumic contraction) (paradoxical ventricular septal motion) represents a qualitative sign of RV volume overload due to severe TR.

**Key point: When TR is more than mild, the evaluation of RV dimensions and function, RA volume, inferior vena cava diameter, and the pulmonary arterial systolic pressure is mandatory.<sup>1</sup> The assessment of RV systolic function using TAPSE and systolic myocardial velocities is reasonable when searching for RV dysfunction; however, they are load dependent and may not reflect true RV myocardial function in severe TR, as well as in patients early after surgery.**

### Integrating indices of severity

The echocardiographic assessment of TR includes integration of data from 2D/3D imaging of the valve, right heart chambers, septal motion, and inferior vena cava as well as Doppler measures of regurgitant severity (Table 9). Colour flow Doppler should be examined in multiple windows. The consensus of the expert is to advocate grading the severity of TR by using the VC width and the PISA radius, except in the presence of mild or trivial TR. However, as extensive data on the usefulness of these approaches are still lacking, corroborating the results of these methods with the other available parameters is also recommended. To note, small physiological degrees of TR are frequently encountered in the normal disease-free individual. The prevalence could reach 65–75%.<sup>1–3</sup> On echocardiography, this 'physiological' TR is associated with normal valve leaflets and no dilatation of either the RV or the RA. Normative values for RA volumes by 3D are now available.<sup>70</sup> It is localized in a small region adjacent to the valve closure (<1 cm), with a thin central jet and often does not extend throughout systole. Peak systolic velocities are between 1.7 and 2.3 m/s.

**Conflict of interest:** none declared.

## References

- Zoghbi WA, Enriquez-Sarano M, Foster E, Grayburn PA, Kraft CD, Levine RA et al. Recommendations for evaluation of the severity of native valvular regurgitation with two-dimensional and Doppler echocardiography. *J Am Soc Echo* 2003;**16**:777–802.
- Lancellotti P, Tribouilloy C, Hagendorff A, Moura L, Popescu BA, Agricola E et al. European Association of Echocardiography. European Association of Echocardiography recommendations for the assessment of valvular regurgitation. Part 1: aortic and pulmonary regurgitation (native valve disease). *Eur J Echocardiogr* 2010;**11**:223–44.
- Lancellotti P, Moura L, Pierard LA, Agricola E, Popescu BA, Tribouilloy C et al. European Association of Echocardiography. European Association of Echocardiography recommendations for the assessment of valvular regurgitation. Part 2: mitral and tricuspid regurgitation (native valve disease). *Eur J Echocardiogr* 2010;**11**:307–32.
- Lang RM, Badano LP, Tsang W, Adams DH, Agricola E, Buck T et al. EAE/ASE recommendations for image acquisition and display using three-dimensional echocardiography. *Eur Heart J Cardiovasc Imaging* 2012;**13**:1–46.
- Carpentier A, Chauvaud S, Fabiani JN, Deloche A, Relland J, Lessana A et al. Reconstructive surgery of mitral valve incompetence: ten-year appraisal. *J Thorac Cardiovasc Surg* 1980;**79**:338–48.
- Vahanian A, Alfieri O, Andreotti F, Antunes M, Baron-Esquivias G, Baumgartner H et al. Guidelines on the management of valvular heart disease (version 2012): the Joint Task Force on the Management of Valvular Heart Disease of the European Society of Cardiology (ESC) and the European Association for Cardio-Thoracic Surgery (EACTS). *Eur Heart J* 2012;**33**:2451–96.
- Pierard LA, Lancellotti P. Stress testing in valve disease. *Heart* 2007;**93**:766–72.
- Muraru D, Badano LP, Vannan M, Illiceto S. Assessment of aortic valve complex by three-dimensional echocardiography: a framework for its effective application in clinical practice. *Eur Heart J Cardiovasc Imaging* 2012;**13**:541–55.
- de Waroux JB, Pouleur AC, Goffinet C, Vancraeynest D, Van Dyck M, Robert A et al. Functional anatomy of aortic regurgitation: accuracy, prediction of surgical reparability, and outcome implications of transesophageal echocardiography. *Circulation* 2007;**116**:1264–9.
- Perry GJ, Helmcke F, Nanda NC, Byard C, Soto B. Evaluation of aortic insufficiency by Doppler colour flow mapping. *J Am Coll Cardiol* 1987;**9**:952–9.
- Tribouilloy CM, Enriquez-Sarano M, Bailey KR, Seward JB, Tajik AJ. Assessment of severity of aortic regurgitation using the width of the vena contracta: a clinical color Doppler imaging study. *Circulation* 2000;**102**:558–64.
- Eren M, Eksik A, Gorgulu S, Norgaz T, Dagdeviren B, Bolca O et al. Determination of vena contracta and its value in evaluating severity of aortic regurgitation. *J Heart Valve Dis* 2002;**11**:567–75.
- Fang L, Hsiung MC, Miller AP, Nanda NC, Yin WH, Young MS et al. Assessment of aortic regurgitation by live three-dimensional transthoracic echocardiographic measurements of vena contracta area: usefulness and validation. *Echocardiography* 2005;**22**:775–81.
- Tribouilloy CM, Enriquez-Sarano M, Fett SL, Bailey KR, Seward JB, Tajik AJ. Application of the proximal flow convergence method to calculate the effective regurgitant orifice area in aortic regurgitation. *J Am Coll Cardiol* 1998;**32**:1032–9.
- Pouleur AC, de Waroux JB, Goffinet C, Vancraeynest D, Pasquet A, Gerber BL et al. Accuracy of the flow convergence method for quantification of aortic regurgitation in patients with central versus eccentric jets. *Am J Cardiol* 2008;**102**:475–80.
- Tribouilloy C, Avinée P, Shen WF, Rey JL, Slama M, Lesbre JP. End diastolic flow velocity just beneath the aortic isthmus assessed by pulsed Doppler echocardiography: a new predictor of the aortic regurgitant fraction. *Br Heart J* 1991;**65**:37–40.
- Samstad SO, Hegrenaes L, Skjaerpe T, Hatle L. Half time of the diastolic aortoventricular pressure difference by continuous wave Doppler ultrasound: a measure of the severity of AR?. *Br Heart J* 1989;**61**:336–43.
- Griffin BP, Flachskampf FA, Siu S, Weyman AE, Thomas JD. The effects of regurgitant orifice size, chamber compliance, and systemic vascular resistance on aortic regurgitant velocity slope and pressure half-time. *Am Heart J* 1991;**122**:1049–56.
- Bouzas B, Kilner PJ, Gatzoulis MA. Pulmonary regurgitation: not a benign lesion. *Eur Heart J* 2005;**26**:433–9.
- Maciel BC, Simpson IA, Valdes-Cruz LM, Recusani F, Hoit B, Dalton N et al. Color flow Doppler mapping studies of 'physiologic' pulmonary and tricuspid regurgitation: evidence for true regurgitation as opposed to a valve closing volume. *J Am Soc Echocardiogr* 1991;**4**:589–97.
- Kobayashi J, Nakano S, Matsuda H, Arisawa J, Kawashima Y. Quantitative evaluation of pulmonary regurgitation after repair of tetralogy of Fallot using real-time flow imaging system. *Jpn Circ J* 1989;**53**:721–7.
- Williams RV, Minich LL, Shaddy RE, Pagotto LT, Tani LY. Comparison of Doppler echocardiography with angiography for determining the severity of pulmonary regurgitation. *Am J Cardiol* 2002;**89**:1438–41.
- Puchalski MD, Askovich B, Sower CT, Williams RV, Minich LL, Tani LY. Pulmonary regurgitation: determining severity by echocardiography and magnetic resonance imaging. *Congenit Heart Dis* 2008;**3**:168–75.

24. Pothineni KR, Wells BJ, Hsiung MC, Nanda NC, Yelamanchili P, Suwanjutha T et al. Live/real time three-dimensional transthoracic echocardiographic assessment of pulmonary regurgitation. *Echocardiography* 2008;**25**:911–7.
25. Goldberg SJ, Allen HD. Quantitative assessment by Doppler echocardiography of pulmonary or aortic regurgitation. *Am J Cardiol* 1985;**56**:131–5.
26. Lei MH, Chen JJ, Ko YL, Cheng JJ, Kuan P, Lien WP. Reappraisal of quantitative evaluation of pulmonary regurgitation and estimation of pulmonary artery pressure by continuous wave Doppler echocardiography. *Cardiology* 1995;**86**:249–56.
27. Silversides CK, Veldtman GR, Crossin J, Merchant N, Webb GD, McGrindle BV et al. Pressure Half-time predicts hemodynamically significant pulmonary regurgitation in adult patients with repaired tetralogy of Fallot. *J Am Soc Echocardiogr* 2003;**16**:1057–62.
28. O'Gara P, Sugeng L, Lang R, Sarano M, Hung J, Raman S et al. The role of imaging in chronic degenerative mitral regurgitation. *JACC Cardiovasc Imaging* 2008;**1**:221–37.
29. Lancellotti P, Lebrun F, Piérard LA. Determinants of exercise-induced changes in mitral regurgitation in patients with coronary artery disease and left ventricular dysfunction. *J Am Coll Cardiol* 2003;**42**:1921–8.
30. Marwick TH, Lancellotti P, Pierard L. Ischaemic mitral regurgitation: mechanisms and diagnosis. *Heart* 2009;**95**:1711–8.
31. Agricola E, Oppizzi M, Pisani M, Meris A, Maisano F, Margonato A. Ischemic mitral regurgitation: mechanisms and echocardiographic classification. *Eur J Echocardiogr* 2008;**9**:207–21.
32. Caldarrera I, Van Herwerden LA, Taams MA, Bos E, Roelandt JR. Multiplane transoesophageal echocardiography and morphology of regurgitant mitral valves in surgical repair. *Eur Heart J* 1995;**16**:999–1006.
33. Lancellotti P, Marwick T, Pierard LA. How to manage ischaemic mitral regurgitation. *Heart* 2008;**94**:1497–502.
34. Omran AS, Woo A, David TE, Feindel CM, Rakowski H, Siu SC. Intraoperative transoesophageal echocardiography accurately predicts mitral valve anatomy and suitability for repair. *J Am Soc Echocardiogr* 2002;**15**:950–7.
35. Kongsarepong V, Shiota M, Gillinov AM, Song JM, Fukuda S, McCarthy PM et al. Echocardiographic predictors of successful versus unsuccessful mitral valve repair in ischemic mitral regurgitation. *Am J Cardiol* 2006;**98**:504–8.
36. Chaliki HP, Nishimura RA, Enriquez-Sarano M, Reeder GS. A simplified, practical approach to assessment of severity of mitral regurgitation by Doppler color flow imaging with proximal convergence: validation with concomitant cardiac catheterization. *Mayo Clin Proc* 1998;**73**:929–35.
37. McCully RB, Enriquez-Sarano M, Tajik AJ, Seward JB. Overestimation of severity of ischemic/functional mitral regurgitation by color Doppler jet area. *Am J Cardiol* 1994;**74**:790–3.
38. Tribouilloy C, Shen WF, Quéré JP, Rey JL, Choquet D, Dufossé H et al. Assessment of severity of mitral regurgitation by measuring regurgitant jet width at its origin with transoesophageal Doppler color flow imaging. *Circulation* 1992;**85**:1248–53.
39. Hall SA, Brickner ME, Willett DL, Irani WN, Afridi I, Grayburn PA. Assessment of mitral regurgitation severity by Doppler color flow mapping of the vena contracta. *Circulation* 1997;**95**:636–42.
40. Matsumura Y, Fukuda S, Tran H, Greenberg NL, Agler DA, Wada N et al. Geometry of the proximal isovelocity surface area in mitral regurgitation by 3-dimensional color Doppler echocardiography: difference between functional mitral regurgitation and prolapse regurgitation. *Am Heart J* 2008;**155**:231–8.
41. Song JM, Kim MJ, Kim YJ, Kang SH, Kim JJ, Kang DH et al. Three-dimensional characteristics of functional mitral regurgitation in patients with severe left ventricular dysfunction: a real-time three-dimensional colour Doppler echocardiography study. *Heart* 2008;**94**:590–6.
42. Yosefy C, Hung J, Chua S, Vaturi M, Ton-Nu TT, Handschumacher MD et al. Direct measurement of vena contracta area by real-time 3-dimensional echocardiography for assessing severity of mitral regurgitation. *Am J Cardiol* 2009;**104**:978–83.
43. Kahlert P, Plicht B, Schenk IM, Janosi RA, Erbel R, Buck T. Direct assessment of size and shape of noncircular vena contracta area in functional versus organic mitral regurgitation using real-time three-dimensional echocardiography. *J Am Soc Echocardiogr* 2008;**21**:912–21.
44. Enriquez-Sarano M, Miller FA Jr, Hayes SN, Bailey KR, Tajik AJ, Seward JB. Effective mitral regurgitant orifice area: clinical use and pitfalls of the proximal isovelocity surface area method. *J Am Coll Cardiol* 1995;**25**:703–9.
45. Lancellotti P, Troisfontaines P, Toussaint AC, Piérard LA. Prognostic importance of exercise-induced changes in mitral regurgitation in patients with chronic ischemic left ventricular dysfunction. *Circulation* 2003;**108**:1713–7.
46. Schwammenthal E, Popescu AC, Popescu BA, Freimark D, Hod H, Eldar M et al. Mechanism of mitral regurgitation in inferior wall acute myocardial infarction. *Am J Cardiol* 2002;**90**:306–9.
47. Iwakura K, Ito H, Kawano S, Okamura A, Kurotobi T, Date M et al. Comparison of orifice area by transthoracic three-dimensional Doppler echocardiography versus proximal isovelocity surface area (PISA) method for assessment of mitral regurgitation. *Am J Cardiol* 2006;**97**:1630–7.
48. Dujardin KS, Enriquez-Sarano M, Bailey KR, Nishimura RA, Seward JB, Tajik AJ. Grading of mitral regurgitation by quantitative Doppler echocardiography: calibration by left ventricular angiography in routine clinical practice. *Circulation* 1997;**96**:3409–15.
49. Tribouilloy C, Shen WF, Rey JL, Adam MC, Lesbre JP. Mitral to aortic velocity-time integral ratio. A non-geometric pulsed-Doppler regurgitant index in isolated pure mitral regurgitation. *Eur Heart J* 1994;**15**:1335–9.
50. Enriquez-Sarano M, Dujardin KS, Tribouilloy CM, Seward JB, Yoganathan AP, Bailey KR et al. Determinants of pulmonary venous flow reversal in mitral regurgitation and its usefulness in determining the severity of regurgitation. *Am J Cardiol* 1999;**83**:535–41.
51. Rogers JH, Bolling SF. The tricuspid valve: current perspective and evolving management of tricuspid regurgitation. *Circulation* 2009;**119**:2718–25.
52. Badano LP, Muraru D, Enriquez-Sarano M. Assessment of functional tricuspid regurgitation. *Eur Heart J* 2013; (Epub ahead of print).
53. Badano LP, Agricola E, Perez de Isla L, Gianfagna P, Zamorano JL. Evaluation of the tricuspid valve morphology and function by transthoracic real-time three-dimensional echocardiography. *Eur J Echocardiogr* 2009;**10**:477–84.
54. Muraru D, Badano LP, Sarais C, Solda E, Illiceto S. Evaluation of tricuspid valve morphology and function by transthoracic three-dimensional echocardiography. *Curr Cardiol Rep* 2011;**13**:242–9.
55. Kim HK, Kim YJ, Park JS, Kim KH, Kim KB, Ahn H et al. Determinants of the severity of functional tricuspid regurgitation. *Am J Cardiol* 2006;**98**:236–42.
56. Kwan J, Kim GC, Jeon MJ, Kim DH, Shiota T, Thomas JD et al. 3D geometry of a normal tricuspid annulus during systole: a comparison study with the mitral annulus using real-time 3D echocardiography. *Eur J Echocardiogr* 2007;**8**:375–83.
57. Matsunaga A, Duran CM. Progression of tricuspid regurgitation after repaired functional ischemic mitral regurgitation. *Circulation* 2005;**112**:1453–7.
58. Fukuda S, Gillinov AM, McCarthy PM, Stewart WJ, Song JM, Kihara T et al. Determinants of recurrent or residual functional tricuspid regurgitation after tricuspid annuloplasty. *Circulation* 2006;**114**:1582–7.
59. Gonzalez-Vilchez F, Zarauza J, Vazquez de Prada JA, Martín Durán R, Ruano J, Delgado C et al. Assessment of tricuspid regurgitation by Doppler color flow imaging: angiographic correlation. *Int J Cardiol* 1994;**44**:275–83.
60. Tribouilloy CM, Enriquez-Sarano M, Bailey KR, Tajik AJ, Seward JB. Quantification of tricuspid regurgitation by measuring the width of the vena contracta with Doppler color flow imaging: a clinical study. *J Am Coll Cardiol* 2000;**36**:472–8.
61. Velayudhan DE, Brown TM, Nanda NC, Patel V, Miller AP, Mehmood F et al. Quantification of tricuspid regurgitation by live three-dimensional transthoracic echocardiographic measurements of vena contracta area. *Echocardiography* 2006;**23**:793–800.
62. Rivera JM, Vandervoort P, Mele D, Weyman A, Thomas JD. Value of proximal regurgitant jet size in tricuspid regurgitation. *Am Heart J* 1996;**131**:742–7.
63. Tribouilloy CM, Enriquez-Sarano M, Capps MA, Bailey KR, Tajik AJ. Contrasting effect of similar effective regurgitant orifice area in mitral and tricuspid regurgitation: a quantitative Doppler echocardiographic study. *J Am Soc Echocardiogr* 2002;**15**:958–65.
64. Grossmann G, Stein M, Kochs M, Höher M, Koenig W, Hombach V et al. Comparison of the proximal flow convergence method and the jet area method for the assessment of the severity of tricuspid regurgitation. *Eur Heart J* 1998;**19**:652–9.
65. Nagueh SF, Kopelen HA, Zoghbi WA. Relation of mean right atrial pressure to echocardiographic and Doppler parameters of right atrial and right ventricular function. *Circulation* 1996;**93**:1160–9.
66. Minagoe S, Rahimtoola SH, Chandraratna PA. Significance of laminar systolic regurgitant flow in patients with tricuspid regurgitation: a combined pulsed-wave, continuous-wave Doppler and two-dimensional echocardiographic study. *Am Heart J* 1990;**119**:627–35.
67. Dini FL, Conti U, Fontanive P, Andreini D, Banti S, Braccini L et al. Right ventricular dysfunction is a major predictor of outcome in patients with moderate to severe mitral regurgitation and left ventricular dysfunction. *Am Heart J* 2007;**154**:172–9.
68. Messika-Zeitoun D, Thomson H, Bellamy M, Scott C, Tribouilloy C, Dearani J et al. Medical and surgical outcome of tricuspid regurgitation caused by flail leaflets. *J Thorac Cardiovasc Surg* 2004;**128**:296–302.
69. Haddad F, Doyle R, Murphy DJ, Hunt SA. Right ventricular function in cardiovascular disease, part II: pathophysiology, clinical importance, and management of right ventricular failure. *Circulation* 2008;**117**:1717–31.
70. Peluso D, Badano LP, Muraru D, Dal Bianco L, Cucchini U, Kocabay G et al. Right atrial size and function assessed with three-dimensional and speckle-tracking echocardiography in 200 healthy volunteers. *Eur Heart J Cardiovasc Imaging* 2013 (Epub ahead of print).